Atmos. Chem. Phys. Discuss., doi:10.5194/acp-2016-883, 2016
Manuscript under review for journal Atmos. Chem. Phys.
Published: 3 November 2016

Atmospheric Chemistry and Physics Discussions

Chemical characterization of fine particular matter in Changzhou, China and source apportionment with offline aerosol mass spectrometry

Zhaolian Ye[1,2], Jiashu Liu[1], Aijun Gu[1], Feifei Feng[1],Yuhai Liu[1], Chenglu Bi[1], Jianzhong Xu[3], Ling Li[2], Hui Chen[2], Yanfang Chen[2], Liang Dai[2], Quanfa Zhou[1], Xinlei Ge[2,*]

[1]College of Chemistry and Environmental Engineering, Jiangsu University of Technology, Changzhou 213001, China
[2]Jiangsu Key Laboratory of Atmospheric Environment Monitoring and Pollution Control, Collaborative Innovation Center of Atmospheric Environment and Equipment Technology, School of Environmental Sciences and Engineering, Nanjing University of Information Science and Technology, Nanjing 210044, China
[3]State Key Laboratory of Cryospheric Sciences, Cold and Arid Regions Environmental and Engineering Research Institute, Chinese Academy of Sciences, Lanzhou 730000, China

*Corresponding author, Email: caxinra@163.com
Phone: +86-25-58731394

Abstract: Knowledge on aerosol chemistry in densely populated regions is critical for reduction of air pollution, while such studies haven't been conducted in Changzhou, an important manufacturing base and polluted city in the Yangtze River Delta (YRD), China. This work, for the first time, performed a thorough chemical characterization on the fine particular matter ($PM_{2.5}$) samples, collected during July 2015 to April 2016 across four seasons in Changzhou city. A suite of analytical techniques were employed to characterize organic carbon/elemental carbon (OC/EC), water-soluble organic carbon (WSOC), water-soluble inorganic ions (WSIIs), trace elements, and polycyclic aromatic hydrocarbons (PAHs) in $PM_{2.5}$; in particular, an Aerodyne soot particle aerosol mass spectrometer (SP-AMS) was deployed to probe the chemical properties of water-soluble organic aerosols (WSOA). The average $PM_{2.5}$ concentrations were found to be 108.3 μg

Atmos. Chem. Phys. Discuss., doi:10.5194/acp-2016-883, 2016
Manuscript under review for journal Atmos. Chem. Phys.
Published: 3 November 2016

Atmospheric Chemistry and Physics Discussions

m^{-3}, and all identified species were able to reconstruct ~80% of the $PM_{2.5}$ mass. The WSIIs occupied about half of the $PM_{2.5}$ mass (~52.1%), with SO_4^{2-}, NO_3^- and NH_4^+ as the major ions. On average, nitrate concentrations dominated over sulfate (mass ratio of 1.21), indicating influences from traffic emissions. OC and EC correlated well with each other and the highest OC/EC ratio (5.16) occurred in winter, suggesting complex OC sources likely including both secondarily formed and primarily emitted OA. Concentrations of eight trace elements (Mn, Zn, Al, B, Cr, Cu, Fe, Pb) can contribute up to 6.0% of $PM_{2.5}$ during winter. PAHs concentrations were also high in winter (140.25 ng m^{-3}), which were predominated by median/high molecular weight PAHs with 5- and 6-rings. The organic matter including both water-soluble and water-insoluble species occupied ~20% $PM_{2.5}$ mass. SP-AMS determined that the WSOA had an average atomic oxygen-to-carbon (O/C), hydrogen-to-carbon (H/C), nitrogen-to-carbon (N/C) and organic matter-to-organic carbon (OM/OC) ratios of 0.36, 1.54, 0.11, and 1.74, respectively. Source apportionment of WSOA further identified two secondary OA (SOA) factors (a less oxidized and a more oxidized OA) and two primary OA (POA) factors (a nitrogen enriched hydrocarbon-like traffic OA and a cooking-related OA). On average, the POA contribution overweighed SOA (55% vs. 45%), indicating the important role of local anthropogenic emissions to the aerosol pollution in Changzhou. Our measurement also shows the abundance of organic nitrogen species in WSOA, and the source analyses suggest these species likely associated with traffic emissions, which warrants more investigations on PM samples from other locations.

1. Introduction

Aerosol particles are ubiquitous in the atmosphere and play important roles in air quality, global climate, biogeochemical cycle, and human health, etc (e.g., Heal et al., 2012;Cao et al., 2012;Hu et al., 2015). Aerosol pollution can also influence remote territories via long-range transport. Therefore, atmospheric aerosol has received extensive attentions from the government, public and academia (e.g., Zhang et al., 2007;Jimenez et al., 2009). Particularly, much attentions have been focused on fine

Atmos. Chem. Phys. Discuss., doi:10.5194/acp-2016-883, 2016
Manuscript under review for journal Atmos. Chem. Phys.
Published: 3 November 2016

Atmospheric Chemistry and Physics Discussions

particles ($PM_{2.5}$, aerodynamic diameters less than 2.5 μm) as they can go deeper into the respiratory system, causing more severe health problems than coarse particles (Anderson et al., 2012). However, as is well known, the concentrations, sources, chemical compositions and formation mechanisms of $PM_{2.5}$ are complicated and can vary greatly with meteorological conditions, seasons and regional/local topography, etc. $PM_{2.5}$ can contain a variety of species, i.e., organic carbon/elemental carbon (OC/EC), trace elements, inorganic salts, and various organic species such as polycyclic aromatic hydrocarbons (PAHs)(e.g., Wang et al., 2015). In China, haze pollution occurred frequently in recent years, and a large number of studies regarding the chemical characterization of fine particles were carried out in many locations (Wang et al., 2006a), such as Shanghai (e.g., Wang et al., 2016a;Zhao et al., 2015), Beijing (e.g., Sun et al., 2014;Hu et al., 2016;Sun et al., 2016), Nanjing (e.g., Zhang et al., 2016;Ding et al., 2013), Lanzhou (e.g., Fan et al., 2014;Xu et al., 2014), Wuhan (e.g., Huang et al., 2016), and other remote sites (Xu et al., 2015), etc.

Yangtze River Delta (YRD) region, located in East China, is experiencing severe atmospheric pollution along with the rapid economic development. Some studies carried out in the YRD investigated different characteristics of the fine aerosols, including the mass loading, composition, hygroscopicity (e.g., Ye et al., 2011;Ge et al., 2015), size distribution, seasonal variation and source, formation pathway, and their impacts on visibility and climate (e.g., Wang et al., 2012). However, these studies were mostly limited in Nanjing (e.g., Hu et al., 2012;Wang et al., 2016b) and Shanghai (e.g., Fu et al., 2012;Qiao et al., 2015;Wang et al., 2012). Changzhou, situated in the western YRD region, between Shanghai and Nanjing, is also a major city and an important manufacturing base due to its geographical advantage. The city has an area of about 4374 km^2 with a population of 4.45 million. Due to elevated emissions of various pollutants, the number of hazy days increased over the past few years in Changzhou as well. To the best of our knowledge, no work has been published specifically on chemical characteristics and source apportionment of fine particles in Changzhou. Thus, it is scientifically and practically important to investigate the $PM_{2.5}$ characteristics in order to

Atmos. Chem. Phys. Discuss., doi:10.5194/acp-2016-883, 2016
Manuscript under review for journal Atmos. Chem. Phys.
Published: 3 November 2016

Atmospheric Chemistry and Physics Discussions

provide efficient control strategies to reduce the PM pollution in Changzhou.

Among various $PM_{2.5}$ constituents, organic aerosol (OA) is a vital component, accounting for a significant, even dominant fraction of $PM_{2.5}$ in ambient air (Zhang et al., 2007). Thus elucidation of its constituents, properties and sources is essential. Apportionment of OA into different sources correctly is a critical step towards enabling efficient air pollution control strategies. Recently, Aerodyne Aerosol Mass spectrometry (AMS) has been used extensively for quantitatively characterizing ambient OA, and the obtained wealthy mass spectral data allows a better source analyses of OA (Canagaratna et al., 2007). Particularly, positive matrix factorization (PMF), as a standard multivariate factor analysis method, has been widely applied on AMS data sets to distinguish and quantify the OA sources (Zhang et al., 2011). Many previous studies (e.g., Ge et al., 2012a;Ng et al., 2011) have deployed the AMS for online field measurements since AMS can provide real-time information on mass concentrations and size distributions of aerosol particles with very fine time resolution (~several minutes). However, up to now, AMS was typically used for short-term online measurement and only a few studies made efforts to apply it on offline filter samples analyses and source apportionment (Ge et al., 2014;Daellenbach et al., 2016;Sun et al., 2011a).

In this study, for the first time, we systematically investigated the chemical characteristics of ambient $PM_{2.5}$ collected in Changzhou nearly across one-year period, providing an overview about the concentrations of $PM_{2.5}$, water-soluble inorganic ions (WSIIs), trace elements, carbonaceous species, water-soluble organic carbon (WSOC), and PAHs in $PM_{2.5}$, and the relationships among these components. Seasonal variations of different $PM_{2.5}$ components were also discussed. Further, we employed an Aerodyne soot particle aerosol mass spectrometer (SP-AMS) (Onasch et al., 2012;Lee et al., 2015;Wang et al., 2016c) to investigate the properties and potential sources of OA on the basis of high resolution mass spectra determined by the SP-AMS. Findings from this study also adds knowledge to the framework of Pan-Eurasian Experiment (PEEX) (Kulmala et al., 2015).

2. Experiments

Atmos. Chem. Phys. Discuss., doi:10.5194/acp-2016-883, 2016
Manuscript under review for journal Atmos. Chem. Phys.
Published: 3 November 2016

Atmospheric Chemistry and Physics Discussions

2.1. Sampling site and $PM_{2.5}$ collection

The sampling site was set on the rooftop of a nine-story building inside the campus of Jiangsu University of Technology in Changzhou (31.7°N, 119.9°E), as shown in Fig. 1. This site locates in the southwestern part of Changzhou, surrounded by a residential area, approximately 0.5 km away from an urban street - Zhongwu Road, and has no direct influences from industrial emissions (14.7 km away from the closest industrial plant– Bao Steel). Meteorological parameters including temperature, relative humidity (RH), wind speed (WS), wind direction (WD), and concentrations of gas-phase species such as SO_2 and NO_2 are recorded by the air quality monitoring station inside the campus, which is about 500 m from the sampling site. Average meteorological parameters of four seasons are shown in Table 1. The wind rose plots of different seasons are shown in Fig. S1 in the supplement. The wind speed was generally low in Changzhou (on average, 1.1, 1.6, 0.9 and 0.8 m s^{-1} in spring, summer, fall and winter, respectively).

$PM_{2.5}$ were collected onto 90 mm quartz fiber filters (Whatman, QM-A) using a medium volume sampler (TH-150 C, Wuhan Tianhong Ltd., China) with a flow rate of 100 L min^{-1}. The filters, wrapped in aluminum foil, were prebaked at 450 °C for 4 h prior to sampling. The sampler began to collect particles at 9:00 am and stopped at 5:00 am in the following day, ensuring the duration time for each sample of 20 h. A total of 69 $PM_{2.5}$ samples were collected in 2015-2016: 20 July - 19 August 2015 (summer, 11 samples), 18 September - 25 October 2015 (fall, 23 samples), 7 December 2015-15 January 2016 (winter, 24 samples) and 1 March -12 April 2016 (spring, 11 samples).

Before and after sampling, the filters were conditioned under constant temperature (22±1°C) and relative humidity (45±5%) for 48 h and weighted by a microbalance (precision of 0.01 mg). The filters were then wrapped and sealed in aluminum foil envelopes separately, stored in a freezer at −20 °C until analysis to minimize the evaporation loss of volatile components.

2.2 Chemical analysis

2.2.1 IC analysis

One quarter of a filter was put into a glass tube and 25 mL deionized water (18.2

Atmos. Chem. Phys. Discuss., doi:10.5194/acp-2016-883, 2016
Manuscript under review for journal Atmos. Chem. Phys.
Published: 3 November 2016

Atmospheric Chemistry and Physics Discussions

147 MΩ cm^{-1}) was then added. After 15 min ultrasonic extraction, the solution was filtrated
148 through an acetate-cellulose filter with 0.45 μm pore size. Concentrations of the WSIIs
149 in the aqueous extract, including five anions (F^-, Cl^-, NO_2^-, NO_3^-, SO_4^{2-}) and five
150 cations (Na^+, NH_4^+, K^+, Mg^{2+}, Ca^{2+}), were then measured by the ion chromatograph (IC,
151 Dionex ICS-600 for anions and ICS-1500 for cations). The method detection limits
152 (MDL) were determined to be 18.0, 7.3, 5.2, 6.3, 11.0, 18.7, 3.3, 4.6, 2.6, and 11.5 μg
153 L^{-1} for F^-, Cl^-, NO_2^-, NO_3^-, SO_4^{2-}, Na^+, NH_4^+, K^+, Mg^{2+} and Ca^{2+}, respectively, and all
154 measured concentrations were above the MDLs. Note the filter blanks were treated in
155 the same way, and all data for the samples reported here were blank corrected, other
156 analyses in the following sections were also blank corrected unless specified. The
157 concentrations of all measured species in $PM_{2.5}$ sample were also converted to μg m^{-3}
158 based on the measured concentrations and the air volume pulled through the filter.

159 **2.2.2 ICP-OES analysis**

160 Another quarter of a filter was cut and placed in a Teflon vessel, digested with 10
161 mL mixture of HNO_3-HCl (1:1, v:v) in a microwave system (XT-9900A, Shanghai
162 Xintuo Co.) for 8 h. After the digested solution cooled down to room temperature, it was
163 filtered through a 0.45 μm acetate-cellulose filter. The filtrate was then diluted using
164 deionized water to 50 mL, and analyzed using Optima 8000 (Perkin Elmer, USA)
165 inductively coupled plasma atomic emission spectrometry (ICP-OES) to determine
166 concentrations of eight trace elements (Mn, Zn, Al, B, Cr, Cu, Fe, Pb). It is worth to
167 mention that we also tried to measure the concentrations of other trace elements such as
168 Ti, Ni, Ba, but found they were mostly below the detection limits thus were not included
169 in this work. All samples were determined in a triplicate, and a difference within 5%
170 was considered acceptable.

171 **2.2.3 OC/EC and WSOC analysis**

172 Analysis procedure of OC/EC was similar to a previous study (Zhao et al., 2015) .
173 Briefly, OC and EC were measured by the DRI model 2001 thermal/optical carbon
174 analyzer (Atmoslytic Inc. Calabasas, CA) using a 0.526 cm^2 punch from each filter,
175 following the IMPROVE TOR protocol (Chow et al., 2004). Filter was measured

Atmos. Chem. Phys. Discuss., doi:10.5194/acp-2016-883, 2016
Manuscript under review for journal Atmos. Chem. Phys.
Published: 3 November 2016

Atmospheric Chemistry and Physics Discussions

stepwise at temperatures of 140 °C (OC_1), 280 °C (OC_2), 480 °C (OC_3), and 580 °C (OC_4) in a helium atmosphere, and 580 °C (EC_1), 740 °C (EC_2), and 840 °C (EC_3) in a 2% oxygen/98% helium gas atmosphere. OC is calculated as OC_1+OC_2+OC_3+OC_4+OP and EC as EC_1+EC_2+EC_3−OP, where OP is the optical pyrolyzed OC.

The WSOC concentrations were determined by a TOC analyzer (TOC-L, Shimazu, Japan). Instrument details and procedure of the WSOC analysis can be found in our previous work (Ge et al., 2014).

2.2.4 GC-MS analysis for PAHs

Due to the limitation of samples, we only analyzed PAHs for spring and winter. The PAHs analysis was conducted following the standard procedure, similar to the work of Szabó et al. (2015). One quarter of a filter was treated by Soxhelt extraction for 18 h using 250 mL mixture of *n*-hexane/ethylether (5:1, v/v). To determine the recovery rates, 100 ng of deuterated surrogate standard solution containing naphthalene-d_8 and perylene-d_{12} (o2si, USA) was added into the sample prior to extraction, and the average recovery rates of d_8 and d_{12} were over 90%. The extracts were then concentrated to about 2 mL by a rotary evaporator, purified in a chromatography column (filled with 3 cm deactivated Al_2O_3, 10g silica gel, 2 cm deactivated Na_2SO_4). The column was first eluted with 25 mL *n*-hexane and the eluate was discarded, then elution was carried out using 30 mL dichloromethane/*n*-hexane (1:1,v:v). Samples containing PAHs were again concentrated to about 2 mL by the rotary evaporation. Finally they were condensed to exactly 1 mL under a gentle N_2 stream in a 60 °C water bath. The extracts are transferred into ampoule bottles and stored in a refrigerator until analysis.

The PAH compounds in the final extracts were analyzed with a gas chromatography - mass spectrometer (GC-MS) (Agilent 7890-7000B, USA), using a DB-5ms capillary column (30 m×0.25 mm×0.5 μm). The instrument conditions were set as follows: injector at 200 °C; ion source at 230 °C; the column was programmed at 40 °C for 2 min, then increased to 100 °C at a rate of 10 °C min^{-1}, held for 1 min, then increased to 250 °C at 20 °C min^{-1}, and finally held for 3 min at 250 °C. The mass selective detector was operated in the electron impact mode using 70 eV. Multi reaction

Atmos. Chem. Phys. Discuss., doi:10.5194/acp-2016-883, 2016
Manuscript under review for journal Atmos. Chem. Phys.
Published: 3 November 2016

Atmospheric Chemistry and Physics Discussions

monitor modes were employed for the identification and quantification of PAHs.

Before sample analysis, calibration standards at a series of concentrations were prepared from aromatic hydrocarbon standard (O2si, USA) containing 18 PAH compounds (1000 mg L^{-1}), which are naphthalene (NaP) ($C_{10}H_8$), acenaphthylene (Acy) ($C_{12}H_8$), acenaphthene (Ace) ($C_{12}H_{10}$), fluorene (Flu) ($C_{13}H_{10}$), phenanthrene (Phe) ($C_{14}H_{10}$), anthracene (Ant) ($C_{14}H_{10}$), fluoranthene (Flua) ($C_{16}H_{10}$), pyrene (Pyr) ($C_{16}H_{10}$), benzo(a)anthracene (BaA) ($C_{18}H_{12}$), chrysene (Chr) ($C_{18}H_{12}$), benzo(b)fluoranthene (BbF) ($C_{20}H_{12}$), benzo(k)fluoranthene (BkF) ($C_{20}H_{12}$), benzo(a)pyrene(BaP) ($C_{20}H_{12}$), Benzo(e)pyrene (BeP) ($C_{20}H_{12}$), benzo(j)fluoranthene (BjF) ($C_{20}H_{12}$), benzo(ghi)perylene (BghiP) ($C_{22}H_{12}$), indeno(1,2,3-cd)pyrene (InP) ($C_{22}H_{12}$), and dibenz(a,h)anthracene (DBA) ($C_{22}H_{14}$). These PAHs can be classified by the number of aromatic rings and molecular weights: low molecular weight (LMW) PAHs containing 2- and 3-rings (NaP, Acy, Ace, Flu, Phe, Ant), medium molecular weight (MMW) PAHs containing 4-rings (Flua, Pyr, BaA, Chr) and high molecular weight (HMW) PAHs containing 5- and 6-rings (BbF, BkF, BjF, BaP, BeP, InP, DBA, BghiP) (Wang et al., 2015;Kong et al., 2015). The calibration was conducted twice prior to analysis. Identification and quantification of each PAH is based on its retention time and peak areas in the calibration curve and sample curve, and the total PAH concentration (Σ PAH) was calculated as the sum of concentrations of all 18 individual PAHs. Figure S2 shows examples of the GC-MS spectra of a few 18-PAHs standards and two surrogate standards (d_8 and d_{12}).

2.2.5 Offline SP-AMS analysis

The SP-AMS analysis procedure for offline filters was similar to that of Xu et al. (2013). Briefly, for each sample, 1/4 filter was extracted in 25 mL deionized water. The liquid extracts were aerosolized using an atomizer (TSI, Model 3076), and the mist passed through a silica-gel diffusion dryer, leaving dry particles which were subsequently analyzed by the SP-AMS. Note the SP-AMS was operated with the laser off so similar to other AMS measurements; it measured non-refractory organic species that can vaporize fast at the oven temperature of 600 ^{o}C. The instrument employs the 70

Atmos. Chem. Phys. Discuss., doi:10.5194/acp-2016-883, 2016
Manuscript under review for journal Atmos. Chem. Phys.
Published: 3 November 2016

eV electron impact (EI) ion generation scheme, all vaporized species were broken into ion fragments with specific mass-to-charge (*m/z*) ratios, and the time-of-flight mass spectrometer outputs the mass spectrum that records the ions according to their signal intensities and *m/z* ratios. Ion fragments with *m/z* up to 300 amu were recorded in this study. The SP-AMS mass spectra can well represent the total OA constituents, and the bulk OA properties such as elemental ratios including oxygen-to-carbon (O/C), hydrogen-to-carbon (H/C) and nitrogen-to-carbon (N/C) ratios, and the organic mass-to-organic carbon (OM/OC) ratio can be obtained. Note although the SP-AMS is limited in molecular-level speciation analysis (Drewnick, 2012), some compounds can be identified via recognition of the fingerprint ions, and particular sources can be separated and quantified via further factor analyses.

The SP-AMS data were processed using the Igor-based software toolkit SQUIRREL (version 1.51H) and PIKA (version 1.10H) (downloaded from: http://cires.colorado.edu/jimenez-group/ToFAMSResources/ToFSoftware/index.html), and the analysis procedure was similar to our previous work (Ge et al., 2012b). We did some minor modifications on the fragment table. For example, we set the organic CO_2^+ signal equal to organic CO^+, as the CO_2^+ signal in $PM_{2.5}$ may come from carbonate not organics, and since we used Argon as carrier gas so different from ambient measurements, the CO^+ signal can be well separated and quantified from N_2^+ at *m/z* 28 (example shown in Fig. S3). Accordingly, organic H_2O^+, HO^+, O^+ were scaled to CO_2^+ using the ratios proposed by Aiken et al. (2008), and the elemental compositions and H/C, N/C, O/C and OM/OC ratios of OA reported in this study were also determined according to the method of Aiken et al. (2008).

2.3 Determination of WSOA, WIOA

Mass concentration of water-soluble organic mass (WSOA) were calculated by multiplying the WSOC concentrations determined from the TOC analyzer with the OM/OC ratios calculated from the SP-AMS mass spectra (Fig. 2) (equation 1). As shown in Fig. 2, most OM/OC values were within the range of 1.4-2.1, in consistent with the typical OM/OC ratios observed at other urban sites.

Atmos. Chem. Phys. Discuss., doi:10.5194/acp-2016-883, 2016
Manuscript under review for journal Atmos. Chem. Phys.
Published: 3 November 2016

The water-insoluble organic carbon (WIOC) mass was calculated as the difference between the OC determined by the OC/EC analyzer and the WSOC, and a factor of 1.3 suggested by Sun et al. (2011a), was used to convert WIOC mass to the mass of water-insoluble organic matter (WIOA) (equation 2). The total organic matter (OA) was treated as the sum of WSOA and WIOA (equation 3).

$$\mathrm{WSOA} = \mathrm{WSOC} \times OM/OC_{WSOA} \quad (1)$$

$$\mathrm{WIOA}=(\mathrm{OC}-\mathrm{WSOC})*1.3 \quad (2)$$

$$\mathrm{OA}=\mathrm{WSOA}+\mathrm{WIOA} \quad (3)$$

2.4 Source apportionment of WSOA

In this work, we used the PMF Evaluation Toolkit v 2.06 (Ulbrich et al., 2009) and followed the protocol described by Zhang et al. (2011) to conduct the PMF analyses. Prior to PMF execution, the following steps were performed: Data and error matrix for WSOA were first adjusted based on equation 1; ions with low signal-to-noise (S/N<0.2) were removed, whereas ions with S/N ratios between 0.2 and 2 were downweighted; Two runs with huge mass loading spikes were removed; all isotopic ions were removed since their signals are not measured directly but scaled to their parent ions. The PMF solutions were explored by varying the factors from 1 to 8 and the rotational forcing parameter (*f*peak) from −1 to 1 with an increment of 0.1. The four-factor solution with *f*peak=0 was chosen as the best solution in this study. The mass spectra of three-factor and five-factor solutions were presented in Fig. S4. The three-factor solution does not resolve well the oxygenated OA factors as many oxygenated ions were mixed with the primary OA factors. The five-factor solution splits the cooking-related OA into two similar factors based on the spectral patterns. Also, by investigating the correlations of the factors with their corresponding tracer ions, and sulfate, nitrate, etc., of the 3-, 4-, and 5-factor solutions, the 4-factor solution was found to be the most reliable and representative solution.

3. Results and discussion

3.1 Overview of $PM_{2.5}$ concentrations and components

Atmos. Chem. Phys. Discuss., doi:10.5194/acp-2016-883, 2016
Manuscript under review for journal Atmos. Chem. Phys.
Published: 3 November 2016

Atmospheric Chemistry and Physics Discussions

The annual and seasonal average concentrations of $PM_{2.5}$, OC, EC, OA, WSIIs, trace elements and PAHs are summarized in Table 2. As shown in Table 2, the $PM_{2.5}$ concentrations (in μg m^{-3}) were on average (±1σ) 106.0 (±24.4), 80.9 (±37.7), 103.3 (±28.2), and 126.9 (±50.4) in spring, summer, fall and winter, respectively, with annual average of 108.3 (±40.8), comparable to the $PM_{2.5}$ concentrations in Nanjing (106 μg m^{-3} in 2011) (Shen et al., 2014), Tianjin (109.8 μg m^{-3} in 2008) (Gu et al., 2010) and Hangzhou (108.2 μg m^{-3} in 2004-2005) (Liu et al., 2015), but lower than that in Jinan (169 μg m^{-3} in 2010) (Gu et al., 2014). The $PM_{2.5}$ concentrations were highest in winter and relatively low in summer, similar to those found in most cities, such as Tianjin (Gu et al., 2010) and Hangzhou (Liu et al., 2015). Previous studies shows that low concentrations occurring in summer are mainly due to the relatively high boundary layer height, low RH and high temperature (Cheng et al., 2015;Huang et al., 2010). The temperatures and RH values were on average 32.1℃ and 61.1% in summer during the observation period (Table 1). Overall, the daily average concentration of $PM_{2.5}$ during sampling period exceeds 75 μg m^{-3} - the second-grade national air quality standard (NAAQS)(GB 3095-2012), and on some heavily polluted days, the $PM_{2.5}$ mass loadings can even exceed 3 times the NAAQS standard.

Table 2 summarizes the concentrations of various species determined in this study. Overall, the reconstructed $PM_{2.5}$ mass estimated by the sum of OA, EC and WSIIs vs gravimetrically determined $PM_{2.5}$ mass were shown in Fig. 3(a-d). The mass proportions of all measured components to the $PM_{2.5}$ mass are illustrated by five inserted pie charts representing four seasons and the whole year, respectively. On average, the quantified species can occupy 77.3% of the $PM_{2.5}$ mass (note trace elements were not included as they were only determined for spring and winter samples), and the mass closure appears to be better for spring and winter samples. Overall, our results are similar to some previous results, such as in Beijing (68%) (Zhang et al., 2013). Details and characteristics of individual components are discussed in the following sections.

3.2 Water soluble inorganic ions

The average concentrations (±σ) of total WSIIs were 66.5 (±17.2), 35.0 (±20.2),

Atmos. Chem. Phys. Discuss., doi:10.5194/acp-2016-883, 2016
Manuscript under review for journal Atmos. Chem. Phys.
Published: 3 November 2016

Atmospheric Chemistry and Physics Discussions

321 51.0 (±17.2), and 66.8 (±23.6) μg m^{-3} in spring, summer, fall and winter, respectively,
322 with an annual average of 56.4 (±22.9) μg m^{-3}. The level was lowest in summer likely
323 due to the conditions favorable for pollutants dispersion and the wet scavenging on these
324 ions under summer monsoon circulation and precipitation. In total, all WSIIs can
325 account for 62.6%, 41.1%, 49.0% and 50.4% of $PM_{2.5}$ mass in spring, summer, fall and
326 winter, respectively, with the annual average WSIIs/$PM_{2.5}$ ratio of 52.1%, a little higher
327 than previously reported value of 45.3% in Handan in 2013 (Meng et al., 2016).

328 The mass fractions of ions to total WSIIs followed the order: NO_3^- (34.2%)> SO_4^{2-}
329 (31.0%)> NH_4^+(21.2%)> Cl^-(6.0%)> Na^+(3.8%)> K^+(1.8%)> Ca^{2+}(1.2%)>
330 Mg^{2+}(0.3%) >NO_2^- and F^-(0.2%) (Fig. 4b). Secondary inorganic ions including SO_4^{2-},
331 NO_3^-, and NH_4^+, constitute the majority of total WSIIs (86.4%) (Fig. 4b) with the
332 highest one being NO_3^-. Nitrate and ammonium concentrations displayed distinct
333 seasonal variations - highest in spring (NO_3^-: 26.4 μg m^{-3}, NH_4^+: 14.8 μg m^{-3}), following
334 by winter (24.1 and 13.1 μg m^{-3}), and lowest in summer (6.8 and 8.2 μg m^{-3}). On the
335 other hand, as a non-volatile species, sulfate concentrations showed no obvious seasonal
336 differences.

337 The cross-correlation relationships between different ions can be used to infer their
338 possible common sources. Figure 5 shows the Pearson's correlation coefficients (r)
339 between ions for four seasons, respectively. As illustrated, NH_4^+ had good correlations
340 with SO_4^{2-} and NO_3^- (r>0.70), and particularly high r values were found in winter (with
341 SO_4^{2-}: r=0.90, with NO_3^-: r=0.96) and summer (with SO_4^{2-}: r=0.98, with NO_3^-: r=0.93),
342 indicating these three ions were mainly present in the form of ammonium nitrate and
343 ammonium sulfate and were all formed secondarily. Moreover, the correlations between
344 Na^+ and Cl^- varied largely with the seasons, poor in summer (r=-0.192) and winter
345 (r=0.37), indicating different sources for them. For chloride, the annual average Cl^-/Na^+
346 mass ratio was 1.58, larger than 1.17 in seawater (Zhang et al., 2013), indicating the
347 important contributions from anthropogenic activities to chloride (such as coal
348 combustion) in Changzhou, in particular in winter as the content of Cl^- in winter was
349 significantly elevated. By contrast, K^+ and Cl^- have good correlations (r of 0.86, 0.76,

Atmos. Chem. Phys. Discuss., doi:10.5194/acp-2016-883, 2016
Manuscript under review for journal Atmos. Chem. Phys.
Published: 3 November 2016

Atmospheric Chemistry and Physics Discussions

0.80 and 0.62 in spring, summer, fall and winter), suggesting that K^+ may co-emit with chloride. According to correlation analysis in Fig. 5, Mg^{2+} and Ca^{2+} had good relations with r of 0.58, 0.80, 0.81 and 0.78 in spring, summer, fall and winter, respectively, indicating a similar source likely crustal material for these two ions.

Acidity of $PM_{2.5}$ can be evaluated by AE (anion equivalence) vs. CE (cation equivalence), which is calculated by converting the concentrations of anions and cations ($\mu g\ m^{-3}$) into molar concentrations ($\mu mol\ m^{-3}$) using the following equations.

$$AE = \frac{SO_4^{2-}}{48} + \frac{NO_3^-}{62} + \frac{NO_2^-}{46} + \frac{Cl^-}{35.5} + \frac{F^-}{19} \quad (4)$$

$$CE = \frac{NH_4^+}{18} + \frac{Mg^{2+}}{12.2} + \frac{Ca^{2+}}{20} + \frac{K^+}{39} + \frac{Na^+}{23} \quad (5)$$

Figure 6a illustrates the scatter plots of CE vs. AE in four seasons. The slopes were 1.18, 1.09, 1.03 and 0.93 in spring, summer, fall and winter, respectively, indicating the particles are generally neutralized. Normally, the ratio of $NH_4^+{}_{meas}$/ $NH_4^+{}_{pred}$, proposed by Young et al. (2016), can be used to evaluate the existing form of NH_4^+ ion. The predicted NH_4^+ ($NH_4^+{}_{pred}$) was calculated using Equation 6.

$$NH_{4\ pred}^+ = 18 \times (2 \times \frac{SO_4^{2-}}{96} + \frac{NO_3^-}{62} + \frac{Cl^-}{35.5}) \quad (6)$$

Figure S5 illustrated the ratio of $NH_{4meas}^+/NH_4^+{}_{pred}$ in $PM_{2.5}$ during four seasons. As presented, the ratios were 0.95, 0.93, 0.87, 0.75 in spring, summer, fall and winter, respectively, indicating that $(NH_4)_2SO_4$ and NH_4NO_3, NH_4Cl were dominant forms for these ionic species. However, the ratio in winter was only 0.75, much less than 1, revealed that the ionic components of $PM_{2.5}$ in winter were more complicated than those in other seasons, reflecting the probability that $PM_{2.5}$ contains other ions such as organic cations in winter.

In addition, the mass ratio of NO_3^- to SO_4^{2-} (NO_3^-/SO_4^{2-}) can be used to identify whether mobile sources (vehicle) or stationary sources (coal combustion) are dominant for these ions (Wang et al., 2006b;Arimoto et al., 1996). When the NO_3^-/SO_4^{2-} mass ratio exceeds 1, it means that particle sources at the observation site are dominated by mobile sources, while fixed sources play major roles when the ratio is below 1. In this

Atmos. Chem. Phys. Discuss., doi:10.5194/acp-2016-883, 2016
Manuscript under review for journal Atmos. Chem. Phys.
Published: 3 November 2016

study, the mass ratios of NO_3^-/SO_4^{2-} in sampling site were 1.52, 0.43, 0.99 and 1.29 in the spring, summer, fall and winter, respectively, with an annual average ratio of 1.21 (Fig. 6b). The NO_3^-/SO_4^{2-} ratio varied largely with seasons. Note in summer, a lower NO_3^-/SO_4^{2-} ratio may be also ascribed to high temperature which leads to the dissociation of NH_4NO_3, yet the high NO_3^-/SO_4^{2-} in winter and spring is more likely relevant to traffic emissions from Zhongwu Road near the sampling site (Fig. 1).

Previous studies (Xu et al., 2014) have indicated that nitrogen oxidation ratio (NOR= $n NO_3^-/(n NO_3^- + n NO_2)$, n refers to the molar concentration), and sulfur oxidation ratio (SOR=$n SO_4^{2-}/(n SO_4^{2-} + n SO_2)$), can be used to estimate the transformation of NO_2 and SO_2 to particle-phase NO_3^- and SO_4^{2-}. The larger SOR and NOR mean more secondarily formed nitrate and sulfate. The seasonal values for SOR and NOR are plotted in Fig. 6 (c-d). The SOR appears to be higher in summer, indicating strong photochemical oxidation for sulfate formation, while NOR is relatively higher in spring, suggesting conversion of NO_x into nitrate is more efficient in spring in Changzhou.

3.3 Trace elements

Eight trace elements (Mn, Zn, Al, B, Cr, Cu, Fe, Pb) of the samples collected during fall and winter were determined in this study. The average concentrations (μg m^{-3}) are shown in Fig. 7a. The total concentrations were 6.38 μg m^{-3} and 2.77 μg m^{-3}, accounting for 6.0% and 3.0% of the total $PM_{2.5}$ mass in winter and fall, respectively. These values were relatively higher than those in other cities in China, such as 1.74%-2.04% in Hangzhou (Liu et al., 2015). This probably can be explained by re-suspended dust from building construction around the site during the sampling period. In this study, the observed mean levels of trace elements in fall were in the order of Fe>Zn>B>Al>Cu>Mn>Pb>Cr, and ranked in Zn>Fe>B>Al>Cu>Mn>Pb>Cr in winter, as demonstrated in Fig. 7a. In fall , Fe accounted for 39.0% of the total trace metal mass, following by Zn (25.6%), B (12.3%) and Al (9.2%), while in winter Zn contributed the largest (53.7%), following by Fe and B. Overall, Fe and Zn were the two most abundant trace elements in $PM_{2.5}$, accounting for over half of the total trace elements mass. Previous research also found that mass loading of Zn was higher than other elements,

Atmos. Chem. Phys. Discuss., doi:10.5194/acp-2016-883, 2016
Manuscript under review for journal Atmos. Chem. Phys.
Published: 3 November 2016

even higher than Al in Nanjing in 2013 (Qi et al., 2016). Vehicle exhaust is likely one major contributor to the high concentrations of Zn.

In general, the correlations between various heavy metals are weak, as depicted in Fig. 7b-d, indicating that the complex sources including both natural and anthropogenic sources for the trace metals observed here. For instance, Cr, Cu, Pb, and Zn can be released from lubricating oils, tail pipe emissions, brake and tire wears (Zhang et al., 2013); Fe and Mg are primarily crustal elements, while Zn and Cu are primarily from anthropogenic sources. Fe and Al were only moderately correlated (for example, in fall with r=0.74, Fig. 7b) showing that they are not from exactly same sources.

3.4 OC and EC

As presented in Table 2, the annual average EC concentration in Changzhou was 5.4 μg m^{-3}, close to Nanjing (5.3 μg m^{-3}) (Li et al., 2015) and Tianjin (5.9 μg m^{-3})(Gu et al., 2010), but lower than those in other cities (e.g., 22.3 μg m^{-3} in Beijing (Duan et al., 2012), and higher than that observed in Shanghai (2.8 μg m^{-3})(Feng et al., 2009). The seasonally averaged OC concentrations were highest in winter (18.3 μg m^{-3}), followed by fall (13.2 μg m^{-3}) and spring (11.2 μg m^{-3}), and lowest in summer (7.9 μg m^{-3}). The annual average OC concentration was 13.8 μg m^{-3}, comparable to those measured in other cities, such as Shanghai (14.7 μg m^{-3})(Feng et al., 2009), and Tianjin (16.9 μg m^{-3}) (Gu et al., 2010).

The mass concentrations of total carbon (TC, the sum of OC and EC) were 16.0, 12.1, 21.0, 22.3 μg m^{-3} in spring, summer, fall and winter, respectively (Table 2), corresponding mass contributions to $PM_{2.5}$ were 15.3%, 17.5%, 19.7%, and 20.1% with an annual mean of 18.1%. This value was similar to those measured in other cities in China, such as Jinan (10-15%)(Gu et al., 2014), Shanghai (15%) (Zhao et al., 2015), and other cities (10-15% in Tianjin, Haining, Zhongshan and Deyang; Zhou et al. (2016)). Organic matter (OA =WSOA+WIOA(μg m^{-3}) exhibited similar seasonal variations as $PM_{2.5}$, and ranked in the order: winter (29.6±11.4) > fall (20.0±11.6)>spring (17.8±3.9)>summer (12.9±1.2). The average mass fraction of OA in $PM_{2.5}$ was 20.3% during the sampling period.

Atmos. Chem. Phys. Discuss., doi:10.5194/acp-2016-883, 2016
Manuscript under review for journal Atmos. Chem. Phys.
Published: 3 November 2016

Atmospheric Chemistry and Physics Discussions

As illustrated in Fig. 8, the OC/EC ratios varied in different seasons and were largest in winter (5.16) followed by spring (2.38), summer (1.88) and fall (1.75). The largest OC/EC ratio occurred in winter, indicating that secondary organic carbon (SOC) was likely a significant component of $PM_{2.5}$ in winter (Chow et al., 2005), however, the high OC/EC ratio may be influenced by biomass burning and/or coal combustion emissions during wintertime too. A number of previous works about the carbonaceous aerosols in the YRD region also showed that highest OC/EC ratio occurred in winter and the ratio was often larger than 2, such as Shanghai (6.35) (Zhao et al., 2015), Nanjing (2.8)(Li et al., 2015), in consistent with our current results in Changzhou.

3.5 PAHs analysis with GC-MS and SP-AMS

The average concentrations of the 18 individual PAH and total PAHs (ΣPAHs) in winter and spring are listed in Table 3. It can be seen that InP (% of total PAHs: 12.6-14.8%), BghiP (10.8–12.3%) and Chr (10.4–11.0%) were the three most abundant PAHs species, followed by BbF (8.69-9.39%), BaP (7.37-8.29%), BeP (5.83-8.61) and BaA (4.53-8.27%). The Σ PAHs in $PM_{2.5}$ were found in the range of 14.0-365.7 ng m^{-3} (mean: 140.25 ng m^{-3}) and 8.9-91.3 ng m^{-3} (mean: 41.42 ng m^{-3}) in winter and spring, respectively. The ΣPAHs concentrations in this study are higher than those reported in Zhenzhou (39 and 111 ng/m^3 in spring and winter)(Wang et al., 2014) and Shanghai (13.7 ng m^{-3} in spring) (Wang et al., 2015), but lower than that reported in many sites of Liaoning Province (75-1900 ng m^{-3}) (Kong et al., 2010). PAHs with medium (4 rings) and high molecular weights (5-6 rings) (MMW and HMW) accounted for the majority of PAHs (88.9% in winter and 79.4% in spring). It is well known that MMW and HMW PAHs are usually associated with coal combustion and vehicular emissions (Wang et al., 2015). Prior study in Nanjing (He et al., 2014) also showed the significant contribution of traffic exhaust to some PAHs including BbF, Chr, Flu, InP, BeP, and BghiP, which in total accounted for more than 53% of the total PAHs.

The diagnostic ratios of selected PAHs including Phe/(Ant+Phe), BaP/BghiP, Flua/(Flua+Pyr), BaP/(BaP+Chr) and Phe/(Ant+Phe) can be used to further distinguish the emission sources of PAHs (Szabó et al., 2015). As suggested previously (Feng et al.,

Atmos. Chem. Phys. Discuss., doi:10.5194/acp-2016-883, 2016
Manuscript under review for journal Atmos. Chem. Phys.
Published: 3 November 2016

Atmospheric Chemistry and Physics Discussions

2015;Saldarriaga-Noreña et al., 2015), traffic source was characterized with a ratio of BaP/BghiP>0.6, and ratios of Flua/(Flua+Pyr) <0.4, 0.4-0.5, >0.5 indicate sources of petrogenic, fossil fuel combustion and coal/wood combustion, respectively. In this work, the Bap/BghiP of 0.61 (winter) and 0.76 (spring) and Flua/(Flua+Pyr) ratios of 0.47 (winter) and 0.50 (spring), all suggest that local vehicular/fossil fuel combustion emissions could be a prominent contributor to particulate PAHs in Changzhou, and contribution from long-range transport was thus minor. Meanwhile, BaP/(BaP+Chr) ratio of 0.40 (winter) and 0.44 (spring) also points to the source from gasoline emission (Khalili et al., 1995). However, the Phe/(Ant+Phe) ratio of 0.89 (winter) and 0.86 (spring) indicate the coal combustion might be also an important source of PAHs.

On the other hand, by using the SP-AMS, we also identified a series of PAH ions, i.e., $C_{16}H_{10}^+$ (*m/z* 202), $C_{17}H_{12}^+$ (*m/z* 216), $C_{18}H_{10}^+$ (*m/z* 226), $C_{18}H_{12}^+$ (*m/z* 228), $C_{19}H_{12}^+$ (*m/z* 240), $C_{19}H_{14}^+$ (*m/z* 242), $C_{20}H_{10}^+$ (*m/z* 250), $C_{20}H_{12}^+$ (*m/z* 252), $C_{21}H_{12}^+$ (*m/z* 264), $C_{21}H_{14}^+$ (*m/z* 266), $C_{22}H_{12}^+$ (*m/z* 276), $C_{23}H_{12}^+$ (*m/z* 288), $C_{23}H_{14}^+$ (*m/z* 290), $C_{24}H_{12}^+$ (*m/z* 300), $C_{24}H_{14}^+$ (*m/z* 302), $C_{25}H_{16}^+$ (*m/z* 316), $C_{26}H_{14}^+$ (*m/z* 326), and $C_{26}H_{16}^+$ (*m/z* 328), as proposed by Dzepina et al. (2007), confirming the existence of PAHs in ambient particles in Changzhou. Note many PAH ions identified by the SP-AMS were not measured by the GC-MS, and the PAH compound DBA which is determined by the GC-MS was not detected by the SP-AMS. This reflects the different sensitivities and responses to the particle-bound PAHs of these two techniques. Table 4 shows the correlation (*r*) coefficients of the concentrations of a few selected PAHs, and the mass ratios of their concentrations measured by both the GC-MS and SP-AMS (results for SP-AMS were based on measurements of all samples, while results for GC-MS were for 23 samples in winter and spring). It can be seen that the concentrations of GC-MS-determined PAHs correlated very well with each other (r>0.92), while the mass loadings determined by the SP-AMS correlated relatively weak. Also, the mass ratios determined from these two instruments were also different. The inconsistencies may be due to the following reasons: (1) the SP-AMS break parent PAH molecules into fragments due to 70 ev EI, thus concentration of a specific PAH ion from the SP-AMS

Atmos. Chem. Phys. Discuss., doi:10.5194/acp-2016-883, 2016
Manuscript under review for journal Atmos. Chem. Phys.
Published: 3 November 2016

cannot represent its corresponding parent PAH compound, while GC-MS determines the concentration of the molecular PAH compound; (2) One PAH ion in the SP-AMS HRMS may be combination of a few PAHs compounds with the same molecular weights; (3) Sensitivities and responses to the trace amount of PAHs of the SP-AMS may be different, thus may lead to uncertainties of the PAHs quantification. Nevertheless, combining GC-MS and SP-AMS to improve the PAH measurements by the SP-AMS is valuable, and will be the subject of our future work.

3.6 Source apportionment of WSOA

3.6.1 WSOA mass spectral profile

To gain further insights into the particulate OA characteristics, we performed the SP-AMS analyses on the water extract of the $PM_{2.5}$ samples, with a focus on OA. The averaged high resolution mass spectra (HRMS) of WSOA classified by six ion categories and five elements are shown in Fig. 9, and the corresponding inset pie charts represent the mass percentages of the ion families and elements, respectively. As illustrated in Fig. 9a, the $C_xH_y^+$ ion family accounts for 38.7% of the WSOA HRMS, followed by $C_xH_yO_2^+$ (28.0%), $C_xH_yN_p^+$ (17.7%) and $C_xH_yO^+$ (10.4%). It is worth to mention that we found that the $C_xH_yN_p^+$ ions contributed significantly, and the organic N (ON) could occupy 8.4% of the total WSOA mass (Fig.9 b). The average concentration of water-soluble organic nitrogen (WSON) over the sampling period was 1.5 μg N m^{-3} (114 nmol N m^{-3}), which is in fact lower than those measured in Beijing (226 nmol N m^{-3}) (Duan et al., 2009), Qingdao (129-199 nmol N m^{-3}) (Shi et al., 2010), Xi,an (300 nmol N m^{-3}) (Ho et al., 2015). The concentration of water-soluble inorganic nitrogen (WSIN, N from ammonium, nitrate and nitrite) was 8.7 μg N m^{-3} base on Table 2, and thus the WSON content corresponds to 14.9% of water-soluble nitrogen (WSN = WSON +WSIN). This values is also lower than those in Beijing (~30%) (Duan et al., 2009), Qingdao (19-22.6%), and Xi,an (22-68%) (Ho et al., 2015).

Nevertheless, the level of ON measured here are a few times higher than those observed in other locations from AMS measurements (typically 1-3%) (Xu et al., 2014), likely due to the following reasons: First, previous studies were online measurements on

Atmos. Chem. Phys. Discuss., doi:10.5194/acp-2016-883, 2016
Manuscript under review for journal Atmos. Chem. Phys.
Published: 3 November 2016

non-refractory submicron aerosols, while it is likely that the supermicron fine particles (1-2.5 μm) contain significant nitrogen-containing species, as observed before for marine aerosols (Violaki and Mihalopoulos, 2010). Secondly, we measured only the water-soluble fraction of OA, which may concentrate more nitrogen-containing species (partially from aqueous-phase processing). Thirdly, a recent study reveals that fossil fuel combustion-related emission can be a dominant source of ammonia in urban area, it thus can act as a significant contributor to amines as amines are often co-emitted with ammonia (Ge et al., 2011b); these amines can be neutralized by inorganic or organic acids and since aminium salts are highly hygroscopic (Ge et al., 2011a), they might be enriched in the WSOA, and generated significant $C_xH_yN_p^+$ ions. Nevertheless, more AMS analyses on the water-extracted $PM_{2.5}$ samples collected from other locations should be conducted to further verify the abundance of ON species in the AMS mass spectra of WSOA.

Overall, the average elemental ratios of the WSOA are 0.36 for O/C, 1.54 for H/C, 0.11 for N/C and 1.74 for OM/OC (Fig. 9a). WSOA is on average comprised of 61.4% C 7.2 % H, 22.9% O, 8.4% N and a negligible fraction (0.2%) of S (Fig. 9b). Except for the enrichment of ON, other results are similar with other online AMS measurement results, such as in Fresno (Ge et al., 2012a).

3.6.2 WSOA sources from PMF analysis

The PMF analysis of the WSOA HRMS matrix identified four OA factors，including two primary OA (POA) factors, named as the nitrogen-enriched hydrocarbon-like OA (NHOA), and cooking-relevant OA (COA), and two secondary OA factors which are a less oxidized oxygenated OA (LO-OOA) and a more oxidized oxygenated OA (MO-OOA), as shown in Fig. 10.

The NHOA factor had a low O/C ratio (0.14), and was abundant in $C_xH_y^+$ ions (33.8%) and the NHOA time series also varied closely with those ions, showing its common feature as traffic OA. In particular, the factor was rich in $C_xH_yN_p^+$ ions (43.1%), as a result, it shows a much higher N/C ratio (0.26, Fig. 10a) than other factors, and correlated well with CHN^+ (r^2=0.82), CH_4N^+ (r^2=0.90), and CH_2N^+ (r^2=0.70), and

Atmos. Chem. Phys. Discuss., doi:10.5194/acp-2016-883, 2016
Manuscript under review for journal Atmos. Chem. Phys.
Published: 3 November 2016

554 $C_2H_4N^+$ (r^2=0.76) (Fig. 10b). The N-containing ions in the NHOA MS were dominated
555 by the reduced ions ($C_xH_yN^+$) rather than oxidized ones ($C_xH_yO_zN^+$), suggesting that
556 amino compounds were likely the major ON species, and was in consistent with our
557 hypothesis aforementioned in Section 3.6.1 that they were mainly from traffic emissions.
558 Nevertheless, future studies should be conducted to investigate in details the
559 contribution of traffic source to the atmospheric ON species.

560 The COA had a low O/C ratio of 0.14 and contained mainly reduced $C_xH_y^+$ ions
561 (60.8%) as well, representing its primary origin. Its mass spectrum is characterized by
562 peaks at *m/z* 55 (significant $C_3H_3O^+$) and *m/z* 57 (significant $C_3H_5O^+$). The abundance of
563 $C_3H_3O^+$ at *m/z* 55 and $C_3H_5O^+$ at *m/z* 57 is a spectral feature of cooking OA, and the
564 overall COA MS and O/C ratios are also similar to the COA factors reported in other
565 studies, such as in Beijing (Sun et al., 2016). The COA time series also correlated well
566 with other cooking-related marker ions, such as $C_5H_8O^+$ (r^2=0.58), $C_6H_{10}O^+$ (r^2 = 0.54),
567 $C_7H_{12}O^+$ (r^2=0.45), consistent with the observations from many previous studies (e.g.,
568 Sun et al., 2011b;Ge et al., 2012a). All these results indicate its feature as
569 cooking-related OA. However, the ratio of COA/$C_6H_{10}O^+$ (622.0) in this study was
570 much higher than that obtained in winter in Fresno and New York City (~180), likely
571 due to we only detected the water-soluble fraction of COA.

572 The LO-OOA MS profile exhibited characteristics of oxidized OA with enhanced
573 signals at *m/z* 29 (CHO^+), *m/z* 43 (mainly $C_2H_3O^+$) and other oxygenated ions. Tight
574 correlations between time series of LO-OOA and CHO^+ (r^2=0.84), and $C_2H_3O^+$ (r^2=0.54)
575 were also observed. Moreover, we also noticed relatively high signals of the BBOA
576 tracer ions $C_2H_4O_2^+$ and $C_3H_5O_2^+$ in the LO-OOA MS, and found good correlations
577 between LO-OOA and BBOA tracers (r^2=0.76 with $C_2H_4O_2^+$, and r^2=0.86 with
578 $C_3H_5O_2^+$), indicating possible influence from biomass burning on the LO-OOA. Thus,
579 we compared mass fraction of LO-OOA to total OA in different seasons assuming that
580 LO-OOA would increase in straw-burning seasons given that it could be influenced by
581 BBOA. Figure S6 showed the mass fraction of four factors during straw-burning seasons
582 (spring, summer) and non-straw burning seasons (fall, winter). No obvious difference

Atmos. Chem. Phys. Discuss., doi:10.5194/acp-2016-883, 2016
Manuscript under review for journal Atmos. Chem. Phys.
Published: 3 November 2016

Atmospheric Chemistry and Physics Discussions

for LO-OOA fraction was found, thus this factor is in fact not heavily influenced by BBOA. Furthermore, the O/C and OM/OC ratios were 0.34 and 1.70, well within the O/C range of less-oxidized OA factors identified in other studies (Jimenez et al., 2009), but beyond the O/C range of typical BBOA (0.18-0.26) (He et al., 2010). On the other hand, the MO-OOA factor had prominent peaks at *m/z* 28 (mainly CO^+) and *m/z* 44 (mainly CO_2^+), and was dominated by $C_xH_yO_1^+$ (36.6%) and $C_xH_yO_2^+$ ions (29.0%) (Fig. 10a). As a result, MO-OOA had a very high O/C ratio of 1.04, showing that it is heavily aged and processed OA component. Correspondingly, its time series correlated well with the secondary OA tracer ions, such as CO_2^+ (r^2=0.87) (Fig. 10b), $C_2H_4O^+$ (r^2=0.45) and $C_2H_3O^+$ (r^2=0.53), etc.

The *f*44 (mass fraction of *m/z* 44 to the total OA) versus *f*43 (mass fraction of *m/z* 43 to the total OA, defined by Ng et al. (2010)), can be used to investigate the degree of oxygenation of the identified factors. As presented in Fig. 11a, apart from NHOA, other three factors (COA, LO-OOA and MO-OOA) all fall within the triangular region. MO-OOA located at the upper position with a higher *f*44 of 0.28, while LO-OOA located at the lower position of plot as it had a high fraction of *f*43 (0.09). This distribution of the four factors is also consistent with other studies.

The mass contributions of the four factors to total WSOA over the whole year are 23.9% for NHOA, 31.2% for COA, 15.3% for LO-OOA and 29.7% for MO-OOA (Fig. 11b). POA (=NHOA+COA) overweighed SOA (=LO-OOA+MO-OOA) mass, showing the dominant role of local anthropogenic emissions to the aerosol pollution in Changzhou, similar to that observed in Nanjing (Wang et al., 2016b). However, during spring and winter, SOA contributions dominate over POA, indicating significant SOA formation in particular the MO-OOA during cold seasons, which is in agreement with the OC/EC results.

4. Conclusions

We presented here the comprehensive characterization results on the $PM_{2.5}$ samples collected across one year in Changzhou City, located in the YRD region of China. The

Atmos. Chem. Phys. Discuss., doi:10.5194/acp-2016-883, 2016
Manuscript under review for journal Atmos. Chem. Phys.
Published: 3 November 2016

Atmospheric Chemistry and Physics Discussions

species we quantified including WSIIs, trace metals, EC, WSOA, WIOA and also PAHs, can reproduce on average ~80% mass of the $PM_{2.5}$ (108.3 μg m^{-3}). WSIIs were the major component, accounting for 52.1% $PM_{2.5}$ mass, and NO_3^-, SO_4^{2-}, NH_4^+ were three most abundant ions. The organic matter (the sum of WSOA and WIOA) occupied ~20% $PM_{2.5}$ mass, and EC accounted for ~5% $PM_{2.5}$ mass. Trace metal elements accounted for ~6% and ~2% $PM_{2.5}$ mass during winter and spring. Total PAHs concentrations were found to be at a relatively high concentration of 140.25 ng m^{-3} in winter, above three times the average mass loading of 41.42 ng m^{-3} in spring, both with InP, BghiP and Chr as the three most abundant PAHs. Average mass ratio of NO_3^-/SO_4^{2-} was 1.21, suggesting a significant role of traffic emissions, which is in consistent with the source analyses results based on the diagnostic ratios of the selected PAHs (BaP/BghiP, Flua/(Flua+Pyr) and BaP/(BaP+Chr)). In addition, a high Cl^-/Na^+ ratio and the diagnostic ratio of Phe/(Ant+Phe) indicated also the contribution from coal combustion, in particular during winter.

In order to obtain further information regarding particle source, we analyzed the WSOA using SP-AMS and conducted PMF analyses on the HRMS of WSOA. Four OA factors including NHOA, COA, LO-OOA and MO-OOA were identified. The mean mass contribution of POA (=NHOA+COA) was larger than that of SOA (=LO-OOA+MO-OOA), revealing that local anthropogenic activities are the major drivers of PM pollution in Changzhou. Nevertheless, during cold seasons, SOA mass contribution increased, indicating significant role of secondarily formed species as well, thus reduction of air pollution in Changzhou should be paid on the strict emission control of both primary particles and the gaseous secondary aerosol precursors. One interesting finding in this work is the enrichment of organic nitrogen species in WSOA, and source analysis indicates that traffic emissions can be a significant contributor to these species, which warrants more detailed investigations in the future. Also, more offline samples should be collected to achieve a more robust PMF analyses. Simultaneous online AMS measurement on the fine particles and measurements of gaseous species (SO_2, NO_2, O_3, CO and some volatile organic compounds) are also

641 essential to better understand the aerosol characteristics, and to implement proper
642 measures to abate the air pollution in this region.
643
644 **Acknowledgements**
645 This work was supported the Natural Science Foundation of China (Grant Nos.
646 (21407079 and 91544220), the Jiangsu National Science Foundation (BK20150042),
647 Specially-Appointed Professors Foundation (for X.G.), the Major Research
648 Development Program of Jiangsu Province (BE2016657 and BY2016030-15), the open
649 fund by Jiangsu Key Laboratory of Atmospheric Environment Monitoring and Pollution
650 Control (KHK1409),. We would also like to acknowledge Mr. Gang Li from Chinese
651 academy of Science for providing us the OC/EC measurements.
652
653 **References:**
654 Aiken, A. C., Decarlo, P. F., Kroll, J. H., Worsnop, D. R., Huffman, J. A., Docherty, K. S.,
655 Ulbrich, I. M., Mohr, C., Kimmel, J. R., Sueper, D., Sun, Y., Zhang, Q., Trimborn, A.,
656 Northway, M., Ziemann, P. J., Canagaratna, M. R., Onasch, T. B., Alfarra, M. R., Prevot, A. S.
657 H., Dommen, J., Duplissy, J., Metzger, A., Baltensperger, U., and Jimenez, J. L.: O/C and
658 OM/OC ratios of primary, secondary, and ambient organic aerosols with high-resolution
659 time-of-flight aerosol mass spectrometry, Environ. Sci. Technol., 42, 4478-4485, doi:
660 10.1021/Es703009q, 2008.

661 Anderson, J. O., Thundiyil, J. G., and Stolbach, A.: Clearing the air: A review of the effects of
662 particulate matter air pollution on human health, J. Med. Toxicol., 8, 166-175, doi:
663 10.1007/s13181-011-0203-1, 2012.

664 Arimoto, R., Duce, R. A., Savoie, D. L., Prospero, J. M., Talbot, R., Cullen, J. D., Tomza, U.,
665 Lewis, N. F., and Ray, B. J.: Relationships among aerosol constituents from Asia and the North
666 Pacific during PEM-West A, J. Geophys. Res. -Atmos., 101, 2011-2023, doi:
667 10.1029/95JD01071, 1996.

668 Canagaratna, M. R., Jayne, J. T., Jimenez, J. L., Allan, J. D., Alfarra, M. R., Zhang, Q., Onasch,
669 T. B., Drewnick, F., Coe, H., Middlebrook, A., Delia, A., Williams, L. R., Trimborn, A. M.,
670 Northway, M. J., DeCarlo, P. F., Kolb, C. E., Davidovits, P., and Worsnop, D. R.: Chemical and
671 microphysical characterization of ambient aerosols with the aerodyne aerosol mass spectrometer,
672 Mass Spectrom Rev, 26, 185-222, doi: 10.1002/Mas.20115, 2007.

673 Cao, J. J., Xu, H. M., Xu, Q., Chen, B. H., and Kan, H. D.: Fine particulate matter constituents
674 and cardiopulmonary mortality in a heavily polluted Chinese city, Environ. Health Persp., 120,
675 373-378, doi: 10.1289/ehp.1103671, 2012.

676 Cheng, Y., He, K. B., Du, Z. Y., Zheng, M., Duan, F. K., and Ma, Y. L.: Humidity plays an
677 important role in the PM(2).(5) pollution in Beijing, Environ. Pollut., 197, 68-75, doi:
678 10.1016/j.envpol.2014.11.028, 2015.

679 Chow, J. C., Watson, J. G., Chen, L. W. A., Arnott, W. P., Moosmüller, H., and Fung, K.:
680 Equivalence of elemental carbon by thermal/optical reflectance and transmittance with different
681 temperature protocols, Environ. Sci. Technol. , 38, 4414-4422, doi: 10.1021/es034936u, 2004.

682 Chow, J. C., Watson, J. G., Louie, P. K., Chen, L. W., and Sin, D.: Comparison of PM2.5 carbon
683 measurement methods in Hong Kong, China, Environ. Pollut., 137, 334-344, doi:
684 10.1016/j.envpol.2005.01.006, 2005.

685 Daellenbach, K. R., Bozzetti, C., Křepelová, A., Canonaco, F., Wolf, R., Zotter, P., Fermo, P.,
686 Crippa, M., Slowik, J. G., Sosedova, Y., Zhang, Y., Huang, R. J., Poulain, L., Szidat, S.,
687 Baltensperger, U., El Haddad, I., and Prévôt, A. S. H.: Characterization and source
688 apportionment of organic aerosol using offline aerosol mass spectrometry, Atmos. Meas. Tech.,
689 9, 23-39, doi: 10.5194/amt-9-23-2016, 2016.

690 Ding, A. J., Fu, C. B., Yang, X. Q., Sun, J. N., Zheng, L. F., Xie, Y. N., Herrmann, E., Nie, W.,
691 Petaja, T., Kerminen, V. M., and Kulmala, M.: Ozone and fine particle in the western Yangtze
692 River Delta: an overview of 1 yr data at the SORPES station, Atmos. Chem. Phys., 13,
693 5813-5830, doi: 10.5194/acp-13-5813-2013, 2013.

694 Drewnick, F.: Speciation analysis in on-line aerosol mass spectrometry, Anal. Bioanal. Chem.,
695 404, 2127-2131, doi: 10.1007/s00216-012-6295-x, 2012.

696 Duan, F., Liu, X., He, K., and Dong, S.: Measurements and characteristics of
697 nitrogen-containing compounds in atmospheric particulate matter in Beijing, China, Bull.
698 Environ. Contam. Toxicol., 82, 332-337, doi: 10.1007/s00128-008-9560-0, 2009.

699 Duan, J., Tan, J., Wang, S., Chai, F., He, K., and Hao, J.: Roadside, urban, and rural comparison
700 of size distribution characteristics of PAHs and carbonaceous components of Beijing, China, J.
701 Atmos. Chem., 69, 337-349, doi: 10.1007/s10874-012-9242-5, 2012.

702 Dzepina, K., Arey, J., Marr, L. C., Worsnop, D. R., Salcedo, D., Zhang, Q., Onasch, T. B.,
703 Molina, L. T., Molina, M. J., and Jimenez, J. L.: Detection of particle-phase polycyclic aromatic
704 hydrocarbons in Mexico City using an aerosol mass spectrometer, Int. J. Mass Spectrom., 263,
705 152-170, doi: 10.1016/j.ijms.2007.01.010, 2007.

706 Fan, J., Yue, X., Jing, Y., Chen, Q., and Wang, S.: Online monitoring of water-soluble ionic
707 composition of PM10 during early summer over Lanzhou City, J. Environ. Sci., 26, 353-361, doi:
708 10.1016/s1001-0742(13)60431-3, 2014.

709 Feng, J., Hu, J., Xu, B., Hu, X., Sun, P., Han, W., Gu, Z., Yu, X., and Wu, M.: Characteristics
710 and seasonal variation of organic matter in PM2.5 at a regional background site of the Yangtze
711 River Delta region, China, Atmos. Environ., 123, 288-297, doi: 10.1016/j.atmosenv.2015.08.019,

712 2015.

713 Feng, Y., Chen, Y., Guo, H., Zhi, G., Xiong, S., Li, J., Sheng, G., and Fu, J.: Characteristics of
714 organic and elemental carbon in PM2.5 samples in Shanghai, China, Atmos. Res., 92, 434-442,
715 doi: 10.1016/j.atmosres.2009.01.003, 2009.

716 Fu, H., Zhang, M., Li, W., Chen, J., Wang, L., Quan, X., and Wang, W.: Morphology,
717 composition and mixing state of individual carbonaceous aerosol in urban Shanghai, Atmos.
718 Chem. Phys., 12, 693-707, doi: 10.5194/acp-12-693-2012, 2012.

719 Ge, X., Wexler, A. S., and Clegg, S. L.: Atmospheric amines - Part II. Thermodynamic
720 properties and gas/particle partitioning, Atmos. Environ., 45, 561-577, doi: DOI
721 10.1016/j.atmosenv.2010.10.013, 2011a.

722 Ge, X., Wexler, A. S., and Clegg, S. L.: Atmospheric amines - Part I. A review, Atmos. Environ.,
723 45, 524-546, doi: DOI 10.1016/j.atmosenv.2010.10.012, 2011b.

724 Ge, X., Setyan, A., Sun, Y., and Zhang, Q.: Primary and secondary organic aerosols in Fresno,
725 California during wintertime: Results from high resolution aerosol mass spectrometry, J.
726 Geophys. Res. -Atmos., 117, D19301, doi: 10.1029/2012jd018026, 2012a.

727 Ge, X., Zhang, Q., Sun, Y., Ruehl, C. R., and Setyan, A.: Effect of aqueous-phase processing on
728 aerosol chemistry and size distributions in Fresno, California, during wintertime, Environ.
729 Chem., 9, 221-235, doi: 10.1071/EN11168, 2012b.

730 Ge, X., Shaw, S. L., and Zhang, Q.: Toward understanding amines and their degradation
731 products from postcombustion CO2 capture processes with aerosol mass spectrometry, Environ.
732 Sci. Technol., 48, 5066-5075, doi: 10.1021/es4056966, 2014.

733 Ge, X., Wang, J., Zhang, Z., Wang, X., and Chen, M.: Thermodynamic modeling of electrolyte
734 solutions by a hybrid ion-interaction and solvation (HIS) model, Calphad, 48, 79-88, doi:
735 10.1016/j.calphad.2014.11.001, 2015.

736 Gu, J., Bai, Z., Liu, A., Wu, L., Xie, Y., Li, W., Dong, H., and Zhang, X.: Characterization of
737 atmospheric organic carbon and element carbon of PM2.5 and PM10 at Tianjin, China, Aerosol
738 Air Qual. Res., 10, 167-176, doi: 10.4209/aaqr.2009.12.0080, 2010.

739 Gu, J., Du, S., Han, D., Hou, L., Yi, J., Xu, J., Liu, G., Han, B., Yang, G., and Bai, Z.-P.: Major
740 chemical compositions, possible sources, and mass closure analysis of PM2.5 in Jinan, China,
741 Air Qual. Atmos. Health, 7, 251-262, doi: 10.1007/s11869-013-0232-9, 2014.

742 He, J., Fan, S., Meng, Q., Sun, Y., Zhang, J., and Zu, F.: Polycyclic aromatic hydrocarbons
743 (PAHs) associated with fine particulate matters in Nanjing, China: Distributions, sources and
744 meteorological influences, Atmos. Environ., 89, 207-215, doi: 10.1016/j.atmosenv.2014.02.042,
745 2014.

746 He, L. Y., Lin, Y., Huang, X. F., Guo, S., Xue, L., Su, Q., Hu, M., Luan, S. J., and Zhang, Y. H.:

747 Characterization of high-resolution aerosol mass spectra of primary organic aerosol emissions
748 from Chinese cooking and biomass burning, Atmos. Chem. Phys., 10, 11535-11543, doi:
749 10.5194/acp-10-11535-2010, 2010.

750 Heal, M. R., Kumar, P., and Harrison, R. M.: Particles, air quality, policy and health, Chem. Soc.
751 Rev., doi, 2012.

752 Ho, K. F., Ho, S. S. H., Huang, R.-J., Liu, S. X., Cao, J.-J., Zhang, T., Chuang, H.-C., Chan, C.
753 S., Hu, D., and Tian, L.: Characteristics of water-soluble organic nitrogen in fine particulate
754 matter in the continental area of China, Atmos. Environ., 106, 252-261, doi:
755 10.1016/j.atmosenv.2015.02.010, 2015.

756 Hu, J., Ying, Q., Wang, Y., and Zhang, H.: Characterizing multi-pollutant air pollution in China:
757 Comparison of three air quality indices, Environ. Int., 84, 17-25, doi:
758 10.1016/j.envint.2015.06.014, 2015.

759 Hu, W., Hu, M., Hu, W., Jimenez, J. L., Yuan, B., Chen, W., Wang, M., Wu, Y., Chen, C.,
760 Wang, Z., Peng, J., Zeng, L., and Shao, M.: Chemical composition, sources, and aging process
761 of submicron aerosols in Beijing: Contrast between summer and winter, J. Geophys. Res.
762 -Atmos., 121, 2015JD024020, doi: 10.1002/2015JD024020, 2016.

763 Hu, X., Zhang, Y., Ding, Z., Wang, T., Lian, H., Sun, Y., and Wu, J.: Bioaccessibility and health
764 risk of arsenic and heavy metals (Cd, Co, Cr, Cu, Ni, Pb, Zn and Mn) in TSP and PM2.5 in
765 Nanjing, China, Atmos. Environ., 57, 146-152, doi: 10.1016/j.atmosenv.2012.04.056, 2012.

766 Huang, T., Chen, J., Zhao, W., Cheng, J., and Cheng, S.: Seasonal variations and correlation
767 analysis of water-soluble inorganic ions in PM2.5 in Wuhan, 2013, Atmosphere, 7, 49, doi:
768 10.3390/atmos7040049, 2016.

769 Huang, X. F., He, L. Y., Hu, M., Canagaratna, M. R., Sun, Y., Zhang, Q., Zhu, T., Xue, L., Zeng,
770 L. W., Liu, X. G., Zhang, Y. H., Jayne, J. T., Ng, N. L., and Worsnop, D. R.: Highly
771 time-resolved chemical characterization of atmospheric submicron particles during 2008 Beijing
772 Olympic Games using an Aerodyne High-Resolution Aerosol Mass Spectrometer, Atmos. Chem.
773 Phys., 10, 8933-8945, doi: 10.5194/acp-10-8933-2010, 2010.

774 Jimenez, J. L., Canagaratna, M. R., Donahue, N. M., Prevot, A. S. H., Zhang, Q., Kroll, J. H.,
775 DeCarlo, P. F., Allan, J. D., Coe, H., Ng, N. L., Aiken, A. C., Docherty, K. S., Ulbrich, I. M.,
776 Grieshop, A. P., Robinson, A. L., Duplissy, J., Smith, J. D., Wilson, K. R., Lanz, V. A., Hueglin,
777 C., Sun, Y. L., Tian, J., Laaksonen, A., Raatikainen, T., Rautiainen, J., Vaattovaara, P., Ehn, M.,
778 Kulmala, M., Tomlinson, J. M., Collins, D. R., Cubison, M. J., Dunlea, E. J., Huffman, J. A.,
779 Onasch, T. B., Alfarra, M. R., Williams, P. I., Bower, K., Kondo, Y., Schneider, J., Drewnick, F.,
780 Borrmann, S., Weimer, S., Demerjian, K., Salcedo, D., Cottrell, L., Griffin, R., Takami, A.,
781 Miyoshi, T., Hatakeyama, S., Shimono, A., Sun, J. Y., Zhang, Y. M., Dzepina, K., Kimmel, J. R.,
782 Sueper, D., Jayne, J. T., Herndon, S. C., Trimborn, A. M., Williams, L. R., Wood, E. C.,
783 Middlebrook, A. M., Kolb, C. E., Baltensperger, U., and Worsnop, D. R.: Evolution of organic
784 aerosols in the atmosphere, Science, 326, 1525-1529, doi: 10.1126/science.1180353, 2009.

785 Khalili, N. R., Scheff, P. A., and Holsen, T. M.: PAH source fingerprints for coke ovens, diesel
786 and, gasoline engines, highway tunnels, and wood combustion emissions, Atmos. Environ., 29,
787 533-542, doi: 10.1016/1352-2310(94)00275-P, 1995.

788 Kong, S., Ding, X., Bai, Z., Han, B., Chen, L., Shi, J., and Li, Z.: A seasonal study of polycyclic
789 aromatic hydrocarbons in PM(2.5) and PM(2.5-10) in five typical cities of Liaoning Province,
790 China, J. Hazard. Mater., 183, 70-80, doi: 10.1016/j.jhazmat.2010.06.107, 2010.

791 Kong, S., Li, X., Li, L., Yin, Y., Chen, K., Yuan, L., Zhang, Y., Shan, Y., and Ji, Y.: Variation
792 of polycyclic aromatic hydrocarbons in atmospheric PM2.5 during winter haze period around
793 2014 Chinese Spring Festival at Nanjing: Insights of source changes, air mass direction and
794 firework particle injection, Sci. Total Environ., 520, 59-72, doi: 10.1016/j.scitotenv.2015.03.001,
795 2015.

796 Kulmala, M., Lappalainen, H. K., Petäjä, T., Kurten, T., Kerminen, V. M., Viisanen, Y., Hari, P.,
797 Sorvari, S., Bäck, J., Bondur, V., Kasimov, N., Kotlyakov, V., Matvienko, G., Baklanov, A.,
798 Guo, H. D., Ding, A., Hansson, H. C., and Zilitinkevich, S.: Introduction: The Pan-Eurasian
799 Experiment (PEEX) – multidisciplinary, multiscale and multicomponent research and
800 capacity-building initiative, Atmos. Chem. Phys., 15, 13085-13096, doi:
801 10.5194/acp-15-13085-2015, 2015.

802 Lee, A. K. Y., Willis, M. D., Healy, R. M., Onasch, T. B., and Abbatt, J. P. D.: Mixing state of
803 carbonaceous aerosol in an urban environment: single particle characterization using the soot
804 particle aerosol mass spectrometer (SP-AMS), Atmos. Chem. Phys., 15, 1823-1841, doi:
805 10.5194/acp-15-1823-2015, 2015.

806 Li, B., Zhang, J., Zhao, Y., Yuan, S., Zhao, Q., Shen, G., and Wu, H.: Seasonal variation of
807 urban carbonaceous aerosols in a typical city Nanjing in Yangtze River Delta, China, Atmos.
808 Environ., 106, 223-231, doi: 10.1016/j.atmosenv.2015.01.064, 2015.

809 Liu, G., Li, J., Wu, D., and Xu, H.: Chemical composition and source apportionment of the
810 ambient PM2.5 in Hangzhou, China, Particuology, 18, 135-143, doi:
811 10.1016/j.partic.2014.03.011, 2015.

812 Meng, C. C., Wang, L. T., Zhang, F. F., Wei, Z., Ma, S. M., Ma, X., and Yang, J.:
813 Characteristics of concentrations and water-soluble inorganic ions in PM2.5 in Handan City,
814 Hebei province, China, Atmos. Res., 171, 133-146, doi: 10.1016/j.atmosres.2015.12.013, 2016.

815 Ng, N. L., Canagaratna, M. R., Zhang, Q., Jimenez, J. L., Tian, J., Ulbrich, I. M., Kroll, J. H.,
816 Docherty, K. S., Chhabra, P. S., Bahreini, R., Murphy, S. M., Seinfeld, J. H., Hildebrandt, L.,
817 Donahue, N. M., DeCarlo, P. F., Lanz, V. A., Prévôt, A. S. H., Dinar, E., Rudich, Y., and
818 Worsnop, D. R.: Organic aerosol components observed in Northern Hemispheric datasets from
819 Aerosol Mass Spectrometry, Atmos. Chem. Phys., 10, 4625-4641, doi:
820 10.5194/acp-10-4625-2010, 2010.

821 Ng, N. L., Canagaratna, M. R., Jimenez, J. L., Zhang, Q., Ulbrich, I. M., and Worsnop, D. R.:

822 Real-time methods for estimating organic component mass concentrations from aerosol mass
823 spectrometer data, Environ. Sci. Technol., 45, 910-916, doi: Doi 10.1021/Es102951k, 2011.

824 Onasch, T. B., Trimborn, A., Fortner, E. C., Jayne, J. T., Kok, G. L., Williams, L. R., Davidovits,
825 P., and Worsnop, D. R.: Soot particle aerosol mass spectrometer: Development, validation, and
826 initial application, Aerosol Sci. Tech., 46, 804-817, doi: 10.1080/02786826.2012.663948, 2012.

827 Qi, L., Zhang, Y., Ma, Y., Chen, M., Ge, X., Ma, Y., Zheng, J., Wang, Z., and Li, S.: Source
828 identification of trace elements in the atmosphere during the second Asian Youth Games in
829 Nanjing, China: Influence of control measures on air quality, Atmos. Pollut. Res., 7, 547-556,
830 doi: 10.1016/j.apr.2016.01.003, 2016.

831 Qiao, T., Zhao, M., Xiu, G., and Yu, J.: Seasonal variations of water soluble composition
832 (WSOC, Hulis and WSIIs) in PM1 and its implications on haze pollution in urban Shanghai,
833 China, Atmos. Environ., 123, 306-314, doi: 10.1016/j.atmosenv.2015.03.010, 2015.

834 Saldarriaga-Noreña, H., López-Márquez, R., Murillo-Tovar, M., Hernández-Mena, L.,
835 Ospina-Noreña, E., Sánchez-Salinas, E., Waliszewski, S., and Montiel-Palma, S.: Analysis of
836 PAHs associated with particulate matter PM2.5 in two places at the city of Cuernavaca, Morelos,
837 México, Atmosphere, 6, 1259-1270, doi: 10.3390/atmos6091259, 2015.

838 Shen, G. F., Yuan, S. Y., Xie, Y. N., Xia, S. J., Li, L., Yao, Y. K., Qiao, Y. Z., Zhang, J., Zhao,
839 Q. Y., Ding, A. J., Li, B., and Wu, H. S.: Ambient levels and temporal variations of PM2.5 and
840 PM10 at a residential site in the mega-city, Nanjing, in the western Yangtze River Delta, China,
841 J. Environ. Sci. Health A: Tox. Hazard. Subst. Environ..Eng., 49, 171-178, doi:
842 10.1080/10934529.2013.838851, 2014.

843 Shi, J., Gao, H., Qi, J., Zhang, J., and Yao, X.: Sources, compositions, and distributions of
844 water-soluble organic nitrogen in aerosols over the China Sea, J. Geophys. Res. -Atmos., 115,
845 doi: 10.1029/2009jd013238, 2010.

846 Sun, Y., Zhang, Q., Zheng, M., Ding, X., Edgerton, E. S., and Wang, X.: Characterization and
847 source apportionment of water-soluble organic matter in atmospheric fine particles (PM2.5) with
848 high-resolution aerosol mass spectrometry and GC-MS, Environ. Sci. Technol., 45, 4854-4861,
849 doi: 10.1021/es200162h, 2011a.

850 Sun, Y., Jiang, Q., Wang, Z., Fu, P., Li, J., Yang, T., and Yin, Y.: Investigation of the sources
851 and evolution processes of severe haze pollution in Beijing in January 2013, J. Geophys. Res.
852 -Atmos., 119, 4380-4398, doi: 10.1002/2014jd021641, 2014.

853 Sun, Y., Du, W., Fu, P., Wang, Q., Li, J., Ge, X., Zhang, Q., Zhu, C., Ren, L., Xu, W., Zhao, J.,
854 Han, T., Worsnop, D. R., and Wang, Z.: Primary and secondary aerosols in Beijing in winter:
855 sources, variations and processes, Atmos. Chem. Phys., 16, 8309-8329, doi:
856 10.5194/acp-16-8309-2016, 2016.

857 Sun, Y. L., Zhang, Q., Schwab, J. J., Demerjian, K. L., Chen, W. N., Bae, M. S., Hung, H. M.,

858 Hogrefe, O., Frank, B., Rattigan, O. V., and Lin, Y. C.: Characterization of the sources and
859 processes of organic and inorganic aerosols in New York city with a high-resolution
860 time-of-flight aerosol mass apectrometer, Atmos. Chem. Phys., 11, 1581-1602, doi:
861 10.5194/acp-11-1581-2011, 2011b.

862 Szabó, J., Nagy, A. S., and Erdős, J.: Ambient concentrations of PM10, PM10-bound polycyclic
863 aromatic hydrocarbons and heavy metals in an urban site of Győr, Hungary, Air Qual. Atmos.
864 Health, 8, 229-241, doi: 10.1007/s11869-015-0318-7, 2015.

865 Ulbrich, I. M., Canagaratna, M. R., Zhang, Q., Worsnop, D. R., and Jimenez, J. L.:
866 Interpretation of organic components from Positive Matrix Factorization of aerosol mass
867 spectrometric data, Atmos. Chem. Phys., 9, 2891-2918, doi: 10.5194/acp-9-2891-2009, 2009.

868 Violaki, K., and Mihalopoulos, N.: Water-soluble organic nitrogen (WSON) in size-segregated
869 atmospheric particles over the Eastern Mediterranean, Atmos. Environ., 44, 4339-4345 doi,
870 2010.

871 Wang, F., Lin, T., Feng, J., Fu, H., and Guo, Z.: Source apportionment of polycyclic aromatic
872 hydrocarbons in PM2.5 using positive matrix factorization modeling in Shanghai, China,
873 Environ. Sci. Process Impacts, 17, 197-205, doi: 10.1039/c4em00570h, 2015.

874 Wang, F., Guo, Z., Lin, T., and Rose, N. L.: Seasonal variation of carbonaceous pollutants in
875 PM2.5 at an urban 'supersite' in Shanghai, China, Chemosphere, 146, 238-244, doi:
876 10.1016/j.chemosphere.2015.12.036, 2016a.

877 Wang, G., Kawamura, K., Lee, S., Ho, K., and Cao, J.: Molecular, seasonal, and spatial
878 distributions of organic aerosols from fourteen Chinese cities, Environ. Sci. Technol., 40,
879 4619-4625, doi: 10.1021/es060291x, 2006a.

880 Wang, J., Geng, N. B., Xu, Y. F., Zhang, W. D., Tang, X. Y., and Zhang, R. Q.: PAHs in $PM_{2.5}$
881 in Zhengzhou: concentration, carcinogenic risk analysis, and source apportionment, Environ.
882 Monit. Assess., 186, 7461-7473, doi: 10.1007/s10661-014-3940-1, 2014.

883 Wang, J., Ge, X., Chen, Y., Shen, Y., Zhang, Q., Sun, Y., Xu, J., Ge, S., Yu, H., and Chen, M.:
884 Highly time-resolved urban aerosol characteristics during springtime in Yangtze River Delta,
885 China: insights from soot particle aerosol mass spectrometry, Atmos. Chem. Phys., 16,
886 9109-9127, doi: 10.5194/acp-16-9109-2016, 2016b.

887 Wang, J., Onasch, T. B., Ge, X., Collier, S., Zhang, Q., Sun, Y., Yu, H., Chen, M., Prévôt, A. S.
888 H., and Worsnop, D. R.: Observation of fullerene foot in eastern China, Environ. Sci. Technol.
889 Lett., 3, 121-126, doi: 10.1021/acs.estlett.6b00044, 2016c.

890 Wang, T., Jiang, F., Deng, J., Shen, Y., Fu, Q., Wang, Q., Fu, Y., Xu, J., and Zhang, D.: Urban
891 air quality and regional haze weather forecast for Yangtze River Delta region, Atmos. Environ.,
892 58, 70-83, doi: 10.1016/j.atmosenv.2012.01.014, 2012.

893 Wang, Y., Zhuang, G., Zhang, X., Huang, K., Xu, C., Tang, A., Chen, J., and An, Z.: The ion

chemistry, seasonal cycle, and sources of PM2.5 and TSP aerosol in Shanghai, Atmos. Environ., 40, 2935-2952, doi: 10.1016/j.atmosenv.2005.12.051, 2006b.

Xu, J., Zhang, Q., Li, X., Ge, X., Xiao, C., Ren, J., and Qin, D.: Dissolved organic matter and inorganic Ions in a central Himalayan glacier—Insights into chemical composition and atmospheric sources, Environ. Sci. Technol., 47, 6181-6188, doi: 10.1021/es4009882, 2013.

Xu, J., Zhang, Q., Chen, M., Ge, X., Ren, J., and Qin, D.: Chemical composition, sources, and processes of urban aerosols during summertime in northwest China: insights from high-resolution aerosol mass spectrometry, Atmos. Chem. Phys., 14, 12593-12611, doi: 10.5194/acp-14-12593-2014, 2014.

Xu, J., Zhang, Q., Wang, Z., Yu, G., Ge, X., and Qin, X.: Chemical composition and size distribution of summertime $PM_{2.5}$ at a high altitude remote location in the northeast of the Qinghai–Xizang (Tibet) Plateau: insights into aerosol sources and processing in free troposphere, Atmos. Chem. Phys., 15, 5069-5081, doi: 10.5194/acp-15-5069-2015, 2015.

Ye, X. N., Ma, Z., Hu, D. W., Yang, X., and Chen, J. M.: Size-resolved hygroscopicity of submicrometer urban aerosols in Shanghai during wintertime, Atmos. Res., 99, 353-364, doi: 10.1016/j.atmosres.2010.11.008, 2011.

Young, D. E., Kim, H., Parworth, C., Zhou, S., Zhang, X., Cappa, C. D., Seco, R., Kim, S., and Zhang, Q.: Influences of emission sources and meteorology on aerosol chemistry in a polluted urban environment: results from DISCOVER-AQ California, Atmos. Chem. Phys., 16, 5427-5451, doi: 10.5194/acp-16-5427-2016, 2016.

Zhang, Q., Jimenez, J. L., Canagaratna, M. R., Allan, J. D., Coe, H., Ulbrich, I., Alfarra, M. R., Takami, A., Middlebrook, A. M., Sun, Y. L., Dzepina, K., Dunlea, E., Docherty, K., DeCarlo, P. F., Salcedo, D., Onasch, T., Jayne, J. T., Miyoshi, T., Shimono, A., Hatakeyama, S., Takegawa, N., Kondo, Y., Schneider, J., Drewnick, F., Borrmann, S., Weimer, S., Demerjian, K., Williams, P., Bower, K., Bahreini, R., Cottrell, L., Griffin, R. J., Rautiainen, J., Sun, J. Y., Zhang, Y. M., and Worsnop, D. R.: Ubiquity and dominance of oxygenated species in organic aerosols in anthropogenically-influenced Northern Hemisphere midlatitudes, Geophys. Res. Lett., 34, n/a-n/a, doi: 10.1029/2007gl029979, 2007.

Zhang, Q., Jimenez, J. L., Canagaratna, M. R., Ulbrich, I. M., Ng, N. L., Worsnop, D. R., and Sun, Y.: Understanding atmospheric organic aerosols via factor analysis of aerosol mass spectrometry: a review, Anal. Bioanal. Chem., 401, 3045-3067, doi: 10.1007/s00216-011-5355-y, 2011.

Zhang, R., Jing, J., Tao, J., Hsu, S. C., Wang, G., Cao, J., Lee, C. S. L., Zhu, L., Chen, Z., Zhao, Y., and Shen, Z.: Chemical characterization and source apportionment of $PM_{2.5}$ in Beijing: seasonal perspective, Atmos. Chem. Phys., 13, 7053-7074, doi: 10.5194/acp-13-7053-2013, 2013.

Zhang, Y. J., Tang, L., Yu, H., Wang, Z., Sun, Y., Qin, W., Chen, W., Chen, C., Ding, A., Wu,

931 J., Ge, S., Chen, C., and Zhou, H.-c.: Chemical composition, sources and evolution processes of
932 aerosol at an urban site in Yangtze River Delta, China during wintertime, Atmos. Environ., 123,
933 339-349, doi: 10.1016/j.atmosenv.2015.08.017, 2016.

934 Zhao, M., Huang, Z., Qiao, T., Zhang, Y., Xiu, G., and Yu, J.: Chemical characterization, the
935 transport pathways and potential sources of $PM_{2.5}$ in Shanghai: Seasonal variations, Atmos. Res.,
936 158-159, 66-78, doi: 10.1016/j.atmosres.2015.02.003, 2015.

937 Zhou, J., Xing, Z., Deng, J., and Du, K.: Characterizing and sourcing ambient $PM_{2.5}$ over key
938 emission regions in China I: Water-soluble ions and carbonaceous fractions, Atmos. Environ.,
939 135, 20-30, doi: 10.1016/j.atmosenv.2016.03.054, 2016.
940
941

Atmos. Chem. Phys. Discuss., doi:10.5194/acp-2016-883, 2016
Manuscript under review for journal Atmos. Chem. Phys.
Published: 3 November 2016

Atmospheric Chemistry and Physics Discussions

942 Table 1. Average meteorological parameters during four seasons

Parameters	Spring	Summer	Fall	Winter
RH (%)	57.3±11.4	61.1±11.8	65.5±10.9	62.3±10.6
T(^{o}C)	13.1±4.0	32.1±4.3	21.6±2.3	5.6±1.8
WS(m s^{-1})	1.1±0.4	1.6±0.6	0.9±0.4	0.8±0.3
WD[a]	SE	E,W,SE	E	W

943 [a] Refer to prevailing wind directions, E—East, SE—Southeast, W—West.

944

945

946

Atmos. Chem. Phys. Discuss., doi:10.5194/acp-2016-883, 2016
Manuscript under review for journal Atmos. Chem. Phys.
Published: 3 November 2016

Atmospheric Chemistry and Physics Discussions

947 Table 2. Summary of the mean concentrations (with one standard deviation) for the $PM_{2.5}$ and all
948 quantified components in four seasons and the whole sampling period.

Species (μg m^{-3})	Spring	Summer	Fall	Winter	Annual
$PM_{2.5}$	**106.0±24.4**	**80.9±37.7**	**103.3±28.2**	**126.9±50.4**	**108.3±40.8**
WSIIs	**66.5±17.2**	**35.0±20.2**	**51.0±17.2**	**66.8±23.6**	**56.4**±22.9
Sulfate	17.3±4.8	15.8±9.8	17.2±6.2	18.7±7.6	17.5±7.1
Nitrate	26.4±8.7	6.8±6.2	17.0±9.0	24.1±11.8	19.3±11.6
Ammonium	14.8±4.2	8.2±4.3	11.2±3.2	13.1±3.7	12.0±4.2
Other ions	8.0±2.3	4.2±2.9	5.6±1.5	10.9±3.4	7.6±3.7
% of $PM_{2.5}$	62.6±4.9	41.1±7.4	49.0±8.5	50.4±7.3	52.1±9.7
TC	**16.0±3.3**	**12.1±1.6**	**21.0±11.8**	**22.3±8.6**	**19.2±9.3**
OC	11.2±2.6	7.9±0.8	13.2±7.8	18.3±8.1	13.8±7.5
EC	4.8±0.9	4.2±1.2	7.7±4.5	4.0±0.9	5.4±3.2
% of $PM_{2.5}$	15.3±2.5	17.5±6.5	19.7±8.2	20.1±3.3	18.1±6.1
OA	**17.8±3.9**	**12.9±1.2**	**20.0±11.6**	**29.6±11.4**	**21.8**±11.3
WSOA	13.1±2.8	11.0±2.2	14.1±6.5	23.4±8.0	16.7±7.9
WIOA	4.8±2.6	1.9±1.8	5.9±7.2	6.1±10.6	5.2±7.6
% of $PM_{2.5}$	17.1±3.0	19.0±7.8	18.7±8.1	23.9±5.5	20.1±7.0
PAHs (ng m^{-3})	**41.42±24.7**			**140.25±60.2**	
Trace elements			**2.77±1.15**	**6.38±3.14**	
OA+EC+WSIIs	**89.1±20.9**	**52.2±21.5**	**81.5±29.6***	**106.8±35.9***	**83.7±32.1**
% of $PM_{2.5}$	**84.2±5.5**	**65.9±4.8**	**78.9±14.9***	**84.2±11.7***	**77.3±11.6**

949 *These values also include contributions from trace elements.
950
951
952
953
954
955
956

Atmos. Chem. Phys. Discuss., doi:10.5194/acp-2016-883, 2016
Manuscript under review for journal Atmos. Chem. Phys.
Published: 3 November 2016

Atmospheric Chemistry and Physics Discussions

957 Table 3. Mean concentration (ng m^{-3}) and mass fractions (%) of individual PAH to the total
958 PAHs.

PAH compounds	Number of rings	Molecular formula and molecular weight (MW)	**Winter**		**Spring**	
			Conc. (ng m^{-3})	% of total	Conc. (ng m^{-3})	% of total
NaP	2-rings	$C_{10}H_8$,128	10.12	7.22	2.60	6.28
Acy		$C_{12}H_8$,152	0.16	0.12	0.08	0.20
Ace		$C_{12}H_{10}$,154	0.15	0.11	0.34	0.83
Flu	3-rings	$C_{13}H_{10}$,166	1.19	0.85	1.70	4.11
Phe		$C_{14}H_{10}$,178	3.54	2.52	3.24	7.83
Ant		$C_{14}H_{10}$,178	0.46	0.33	0.54	1.31
Flua		$C_{16}H_{10}$,202	8.05	5.74	2.57	6.21
Pyr		$C_{16}H_{10}$,202	8.93	6.37	2.43	5.87
BaA	4-rings	$C_{18}H_{12}$, 228	11.6	8.27	1.88	4.53
Chr		$C_{18}H_{12}$, 228	15.41	11.0	4.32	10.43
BbF+BjF		$C_{20}H_{12}$, 252	12.19	8.69	3.89	9.39
BkF		$C_{20}H_{12}$, 252	5.58	3.98	1.87	4.50
BaP	5-rings	$C_{20}H_{12}$, 252	10.33	7.37	3.43	8.29
BeP		$C_{20}H_{12}$, 252	12.08	8.61	2.42	5.83
DBA		$C_{22}H_{14}$, 278	2.53	1.8	0.42	1.02
InP	6-rings	$C_{22}H_{12}$, 276	20.74	14.8	5.23	12.62
BghiP		$C_{22}H_{12}$, 276	17.18	12.3	4.46	10.76
LMW-PAHs	2-3 rings		15.62	11.1	8.50	20.6
MMW-PAHs	4-rings		43.99	31.4	11.20	27.0
HMW-PAHs	5-6 rings		80.63	57.5	21.72	52.4
ΣPAHs			140.25	100.0	41.42	100.0

959

Atmos. Chem. Phys. Discuss., doi:10.5194/acp-2016-883, 2016
Manuscript under review for journal Atmos. Chem. Phys.
Published: 3 November 2016

Atmospheric Chemistry and Physics Discussions

960 Table 4 Cross-correlation coefficients (*r*) of the measured concentrations of the PAH speciesand
961 ratios of the mean concentrations between these species from GC-MS (bold) and SP-AMS
962 (itlaic).

PAHs	$C_{16}H_{10}$	$C_{18}H_{12}$	$C_{20}H_{12}$	$C_{22}H_{12}$	Ratio (GC)	Ratio (SP-AMS)
$C_{16}H_{10}$	1	*-0.250*	*-0.062*	*-0.140*	**$C_{16}H_{10}/C_{16}H_{10}$=1**	*$C_{16}H_{10}^{+}/C_{16}H_{10}^{+}$=1*
$C_{18}H_{12}$	**0.952**	**1**	*0.572*	*0.528*	**$C_{16}H_{10}/C_{18}H_{12}$=0.84**	*$C_{16}H_{10}^{+}/C_{18}H_{12}^{+}$=0.43*
$C_{20}H_{12}$	**0.936**	**0.994**	1	*0.771*	**$C_{16}H_{10}/C_{20}H_{12}$=0.36**	*$C_{16}H_{10}^{+}/C_{20}H_{12}^{+}$=0.56*
$C_{22}H_{12}$	**0.925**	**0.986**	**0.993**	1	**$C_{16}H_{10}/C_{22}H_{12}$=0.35**	*$C_{16}H_{10}^{+}/C_{22}H_{12}^{+}$=1.17*

963 $C_{16}H_{10}$: Flua+Pyr; $C_{18}H_{10}$: BaA+Chr; $C_{20}H_{12}$: BbF+BjF+BkF+BaP+BeP;
964 $C_{22}H_{12}$: BghiP+InP+DBA
965

Atmos. Chem. Phys. Discuss., doi:10.5194/acp-2016-883, 2016
Manuscript under review for journal Atmos. Chem. Phys.
Published: 3 November 2016

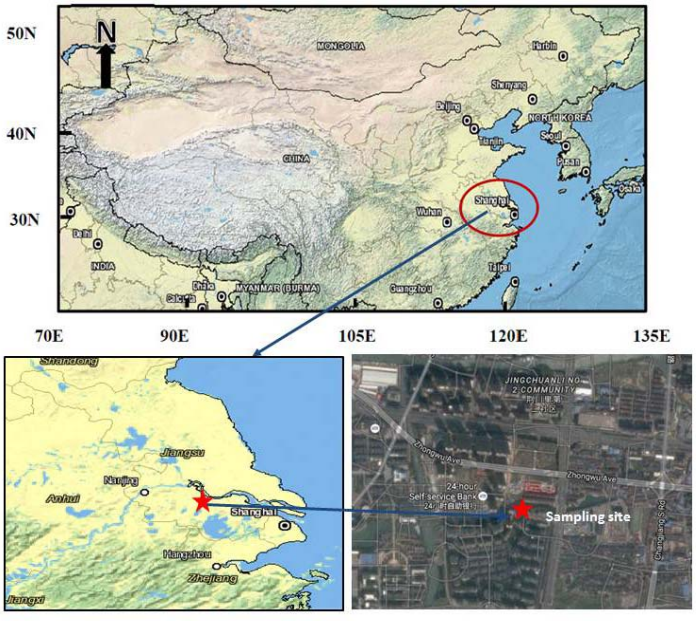

Figure 1. Schematic map of the sampling site, its surroundings and location.

Atmos. Chem. Phys. Discuss., doi:10.5194/acp-2016-883, 2016
Manuscript under review for journal Atmos. Chem. Phys.
Published: 3 November 2016

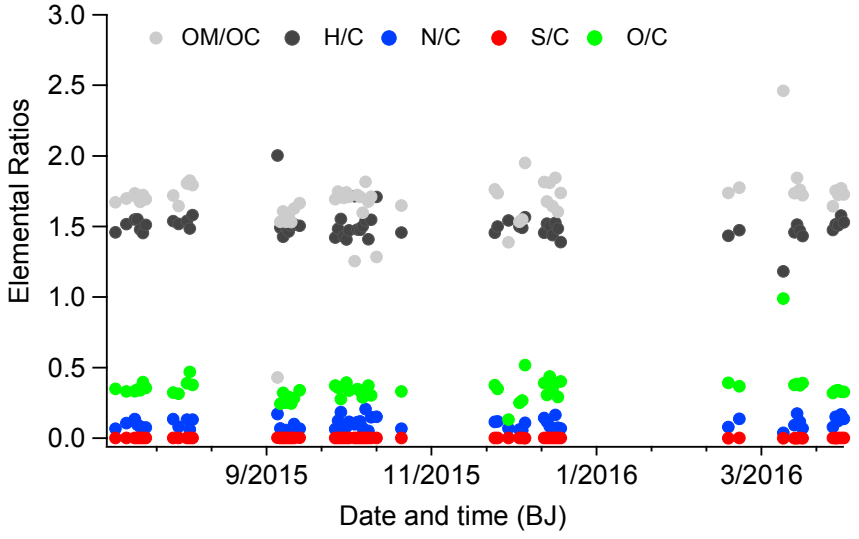

970

971 Figure 2. The atomic elemental ratios for the water-soluble organic matter (WSOA) determined

972 by the SP-AMS.

973

974

975

976

Atmos. Chem. Phys. Discuss., doi:10.5194/acp-2016-883, 2016
Manuscript under review for journal Atmos. Chem. Phys.
Published: 3 November 2016

Atmospheric Chemistry and Physics Discussions

977

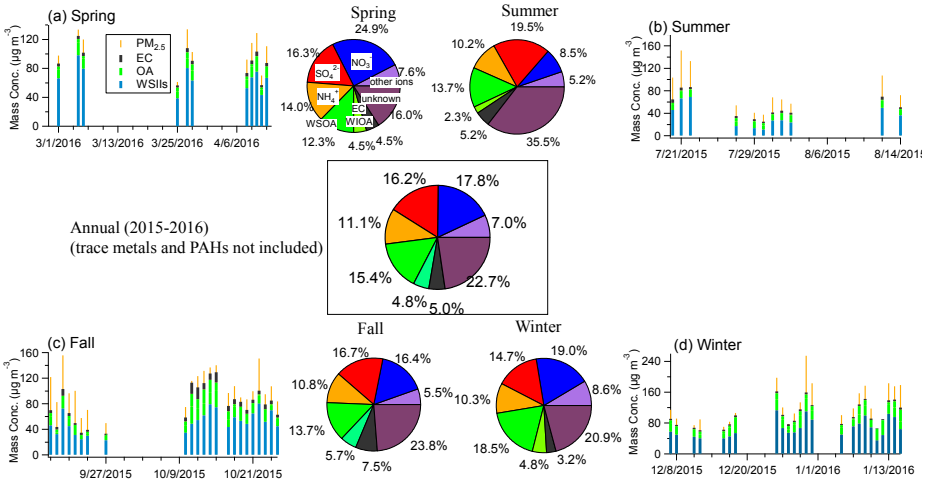

978

979

980 Figure 3. Reconstructed mass (=OA+EC+WSIIs) vs. $PM_{2.5}$ mass from gravimetric measurement
981 ($PM_{2.5}$) in (a) sping, (b) summer, (c) fall, (d) winter, and annual. Corresponding pie charts show
982 the mass percentages of different species to the $PM_{2.5}$ mass (trace elements and PAHs are not
983 included due to sample limitations).

984

Atmos. Chem. Phys. Discuss., doi:10.5194/acp-2016-883, 2016
Manuscript under review for journal Atmos. Chem. Phys.
Published: 3 November 2016

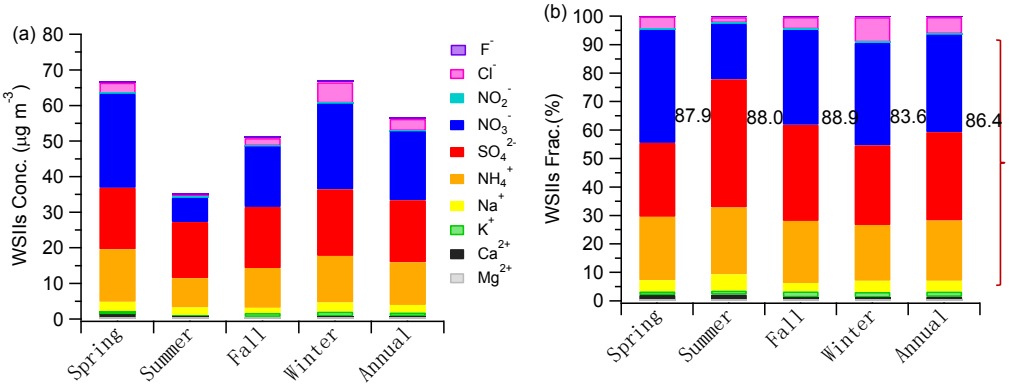

985
986

987 Figure 4. (a) Seasonal variations of average mass concentrations and (b) mass fractional
988 contributions of WSIIs in $PM_{2.5}$ in Changzhou during 2015-2016. The values marked in (b) are
989 the fractions of three major ions (NO_3^-+SO_4^{2-}+NH_4^+) to the total WSIIs.
990

Atmos. Chem. Phys. Discuss., doi:10.5194/acp-2016-883, 2016
Manuscript under review for journal Atmos. Chem. Phys.
Published: 3 November 2016

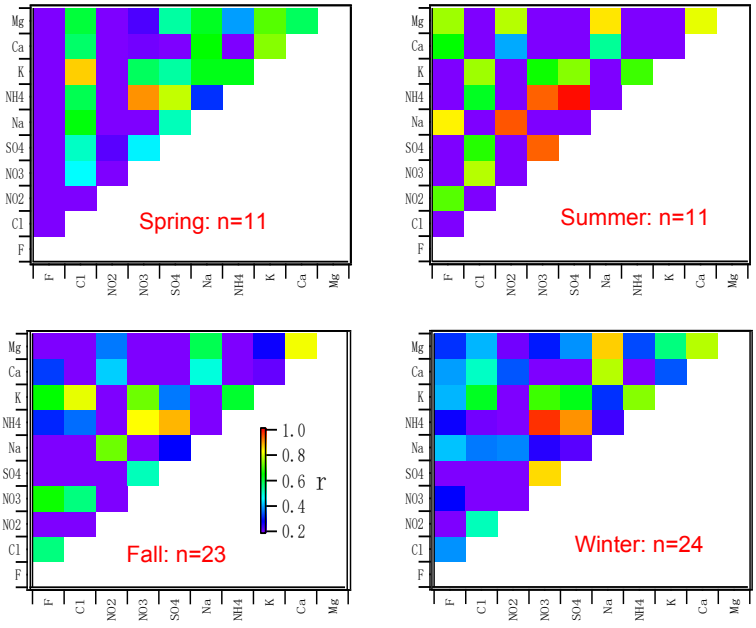

991

992 Figure 5. Image plots showing the cross correlation coefficients between water-soluble ions in

993 $PM_{2.5}$ in four seasons. Boxes are colored by correlations (*r*).

994

Atmos. Chem. Phys. Discuss., doi:10.5194/acp-2016-883, 2016
Manuscript under review for journal Atmos. Chem. Phys.
Published: 3 November 2016

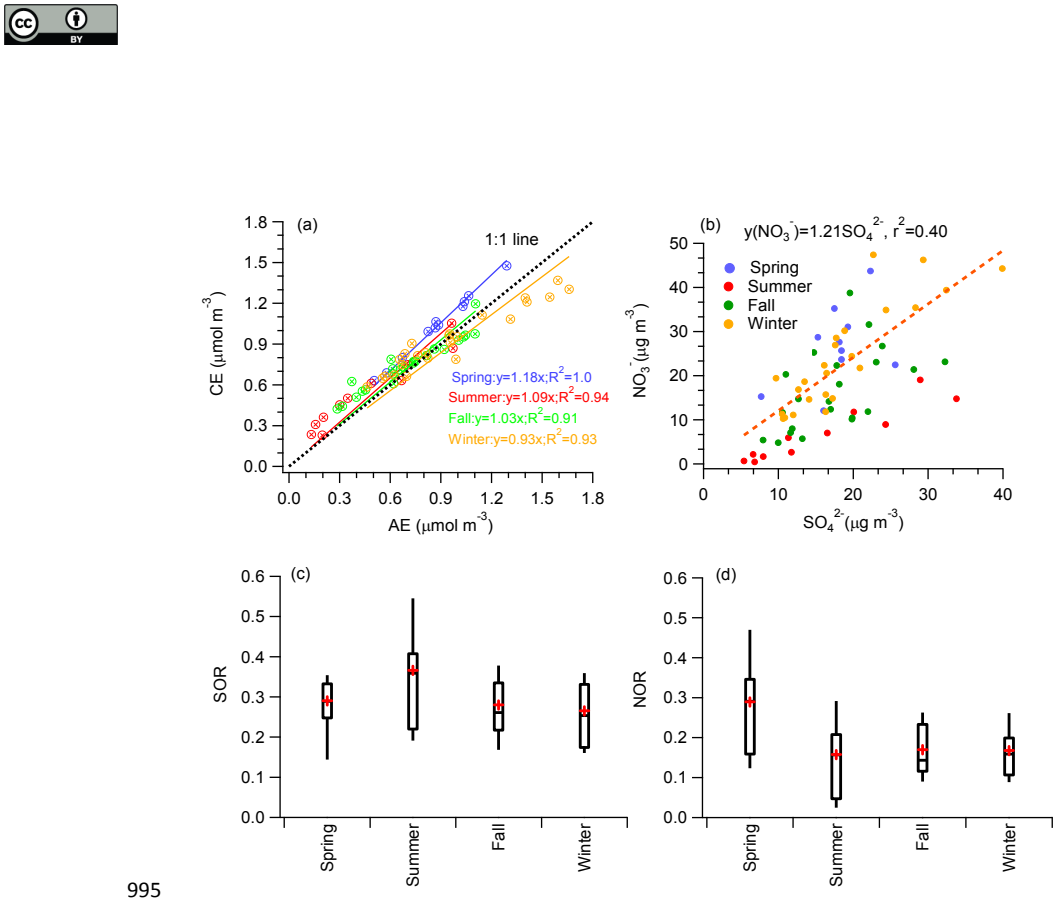

Figure 6. (a) Scatter plots of molar concentrations of cations vs. anions, (b) scatter plots of NO_3^- vs. SO_4^{2-} concentrations, (c-d) SOR and NOR value during four seasons. In (a), the dashed line refers to 1:1 line. In (b), the dashed line was the averaged fitted line, representing NO_3^-/SO_4^{2-} ratio during the entire period. Data in different season are shown by different colors for comparison. Linear regression equations were also presented. In (c-d), the crosses represent the mean, the middle bars represent the median, the top and bottom of the box represents the 75th and 25th percentile, respectively, and the top and bottom whiskers represent the 90th and 10th percentile, respectively.

Atmos. Chem. Phys. Discuss., doi:10.5194/acp-2016-883, 2016
Manuscript under review for journal Atmos. Chem. Phys.
Published: 3 November 2016

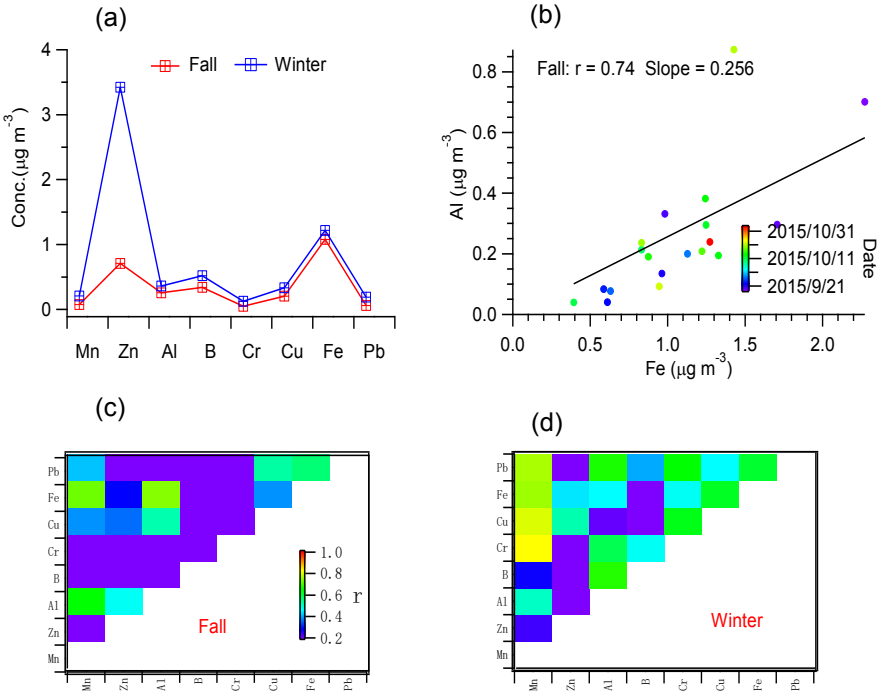

Figure 7. (a) Mean mass concentrations of trace elements determined for fall and winter, (b) Scatter plots of Al and Fe in fall, and (c-d) cross-correlation coefficients (*r*) among different trace elements in fall and winter, respectively.

Atmos. Chem. Phys. Discuss., doi:10.5194/acp-2016-883, 2016
Manuscript under review for journal Atmos. Chem. Phys.
Published: 3 November 2016

Atmospheric Chemistry and Physics Discussions

1011

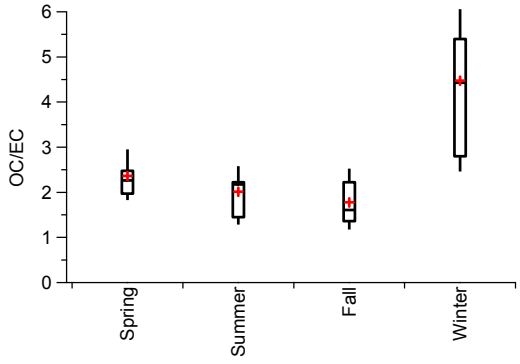

1012

1013 Figure 8. Average OC/EC ratios measured in four seasons (symbols of the box plots are the
1014 same as described in Figure 6.)

1015

Atmos. Chem. Phys. Discuss., doi:10.5194/acp-2016-883, 2016
Manuscript under review for journal Atmos. Chem. Phys.
Published: 3 November 2016

Atmospheric Chemistry and Physics Discussions

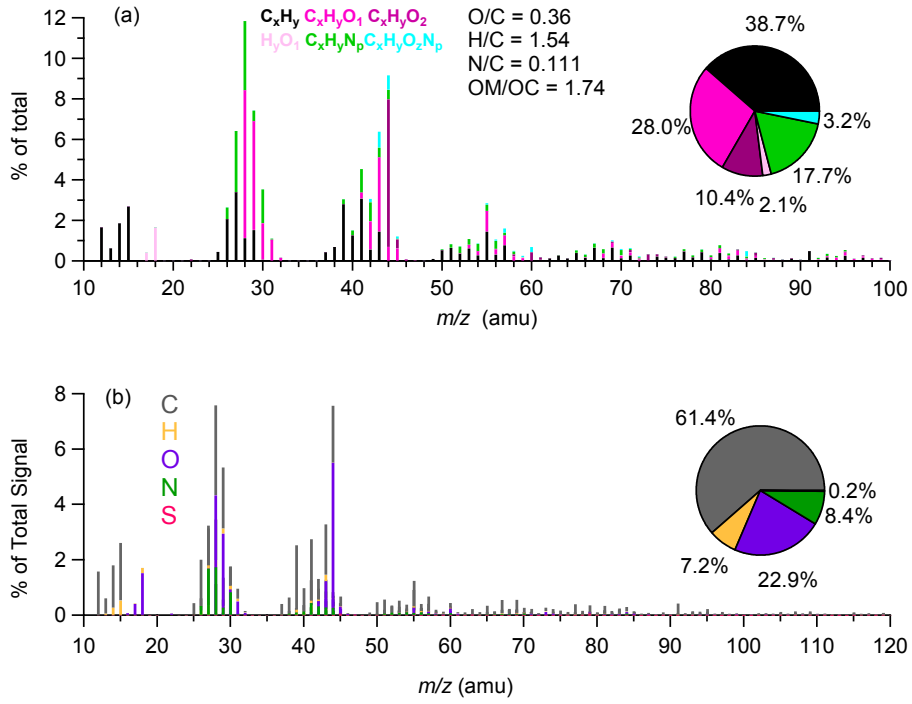

Figure 9. (a) High-resolution mass spectral profile of the WSOA measured by the SP-AMS (Mass spectrum is classified and colored by six ion families; pie chart shows the mass contributions of each ion family to the total MS), (b) Average mass spectrum classified by five elements (C, H, O, N, and S) (inset pie chart shows mass contributions of the five elements, respectively).

Atmos. Chem. Phys. Discuss., doi:10.5194/acp-2016-883, 2016
Manuscript under review for journal Atmos. Chem. Phys.
Published: 3 November 2016

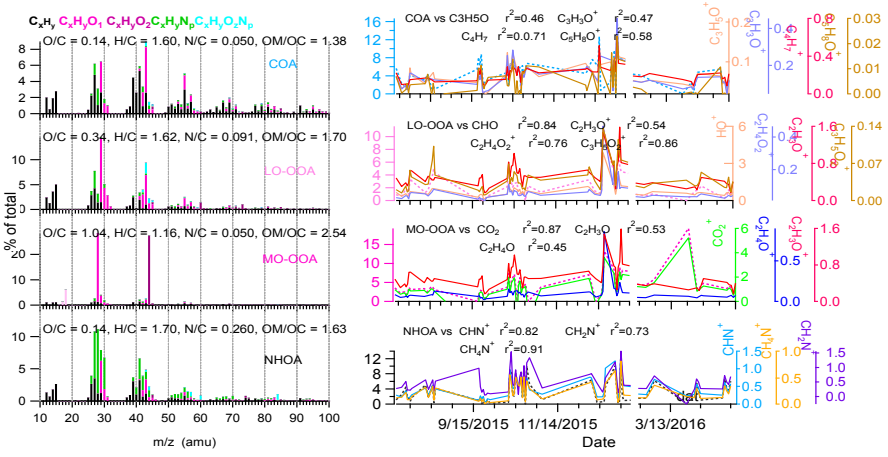

Figure 10. (a) High-resolution mass spectra of nitrogen-enriched hydrocarbon-like OA (NHOA), cooking-related OA (COA), less-oxidized OA (LO-OOA) and more-oxidized OA (MO-OOA) separated by the PMF analyses, colored by six ion categories, (b) time series of the four WSOA factors, and corresponding tracer ions.

Atmos. Chem. Phys. Discuss., doi:10.5194/acp-2016-883, 2016
Manuscript under review for journal Atmos. Chem. Phys.
Published: 3 November 2016

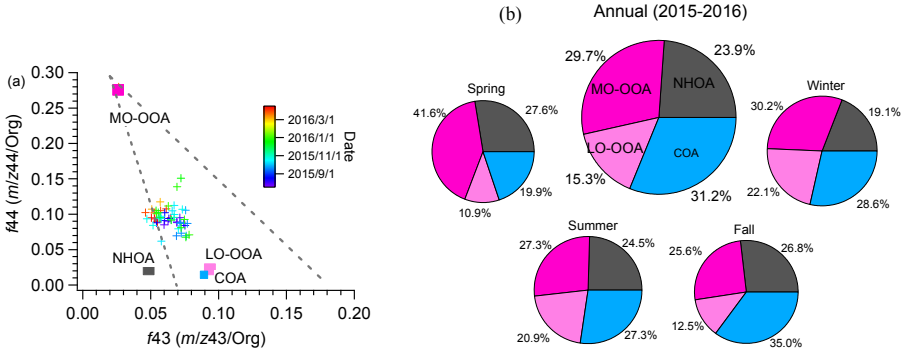

Figure 11. (a) Triangle plot of *f*44 *vs.* *f*43 for all WSOA, and the four WSOA factors identified by the PMF analyses, (b) pie charts of the mass contributions of four WSOA factors to the total WSOA in four seasons and the whole sampling period.